Hydrol. Earth Syst. Sci., 30, 5947–5970, 2026
https://doi.org/10.5194/hess-30-5947-2026

Hydrology and Earth System Sciences
Open Access

Characterising runoff processes for Australia: insights from a parsimonious rainfall-runoff event identification method

Mohammad Masoud Mohammadpour Khoie[1,2], **Danlu Guo**[1,2], **and Conrad Wasko**[3]

[1]School of Engineering, ANU College of Systems and Society, Australian National University, Canberra, Australian Capital Territory, Australia
[2]Institute for Water Futures, The Australian National University, Canberra, Australian Capital Territory, Australia
[3]School of Civil Engineering, The University of Sydney, Sydney, New South Wales, Australia

Correspondence: Mohammad Masoud Mohammadpour Khoie (masoud.mohammadpour@anu.edu.au)

Received: 15 December 2025 – Discussion started: 5 February 2026
Revised: 31 July 2026 – Accepted: 21 August 2026 – Published: 23 September 2026

Abstract. Rainfall-runoff events are widely used in hydrological applications, from flood estimation and flood forecasting, to understanding catchment responses in a climate/anthropogenic affected world. The majority of methods used to identify rainfall-runoff events are statistical in nature, relying on subjective, user-defined "rules" (i.e., parameters) that define a rainfall-runoff event. Since no ground-truth information is available to confirm the exact beginning and end of rainfall-runoff events, there is noticeable inconsistency (i.e. uncertainty) within the results. In this study, we propose the Robust Variance-based Event Identification Method (RVEIM), a new parsimonious rainfall-runoff event identification method which uses fewer parameters and better mimics the natural runoff generation process; decreasing the uncertainty in rainfall-runoff event identification. RVEIM detects runoff events by focusing on changes of streamflow variance and pairs to the corresponding rainfall event(s) simultaneously. RVEIM was compared to two benchmarking event identification methods in 8 representative catchments in Australia. A sensitivity analysis was performed using a comprehensive set of plausible event identification parameter values for all methods. Results revealed that the variation of rainfall-runoff events characteristics – including annual number, length, and the mean of paired runoff events – showed limited uncertainty from the RVEIM (standard deviation within $\pm 15\,\%$ of the mean across 8 representative Australian catchments). In contrast, the two benchmarking methods exhibited substantially higher uncertainties (43 % to 93 %). Using RVEIM, we present the first comprehensive summary of rainfall-runoff event characteristics across 467 Australian catchments. The distribution of event-scale runoff coefficients for individual catchments shows a strong climate gradient. Such systematic shifts in the distribution of runoff coefficient across climate regions indicate that climate variables play an important role in catchment response and point to potential contrasts in dominating runoff generation mechanisms across climate zones.

1 Introduction

Event-based rainfall-runoff analyses provide insights into the catchment response and promote the understanding of streamflow processes (Fischer and Schumann, 2024; Tang and Carey, 2017; Tarasova et al., 2020; Tarasova et al., 2018b; Wasko and Guo, 2022). Streamflow and rainfall timeseries are analysed to identify independent events, which are then paired to characterize rainfall-runoff events. Characteristics such as the number, duration, volume, and Runoff Coefficient (RC, the ratio of rainfall contributing to runoff) are commonly assessed to understand rainfall-runoff relationships and the dynamics of catchment response. Event-based rainfall-runoff analyses have hence been widely used to explore hydrological processes and to assess the impact of both anthropogenic and climatic change (Ho et al., 2022; Sriwongsitanon and Taesombat, 2011; Hu et al., 2021; Merz and Blöschl, 2009; Chen et al., 2020; Sillanpää and Koivusalo, 2015; Wu et al., 2025; Wang et al., 2012).

For example, Tarasova et al. (2018a) used rainfall-runoff event identification methods to recognize regional patterns

Published by Copernicus Publications on behalf of the European Geosciences Union.

of rainfall-runoff events in Germany. Their results showed that subsurface properties significantly contribute to runoff response. Merz et al. (2006) identified rainfall-runoff events and analysed RCs across Austria. They showed that the RC is spatially correlated with mean annual precipitation, soil type, and land use. By analysing rainfall-runoff events characteristics, Merz et al. (2006) also reported that the RC is a function of the current and previous rainfall event. Similarly, Rahi et al. (2023) studied the trends of RCs and its drivers in the Upper Tiber basin, Italy. They showed that RC has experienced a decreasing trend from 1927–2020 while the air temperature has increased. They also noted that, among hydroclimate variables, RC showed the strongest correlations with soil water storage. In the Huanghe River basin China, Chen et al. (2007) reported that annual RC is positively correlated with precipitation and negatively correlated with temperature. Ho et al. (2022) further showed that the RC of flood events in Australia exhibit regionally varying trends under climate change. Together, these studies highlight the utility of event-based analysis in identifying regional hydroclimatic patterns, catchment runoff drivers, as well as detecting long-term changes in rainfall-runoff dynamics.

Several rainfall-runoff event identification methods have been proposed in the literature (Tang and Carey, 2017; Merz et al., 2006; Kaur et al., 2017; Fischer et al., 2021; Giani et al., 2022; Koskelo et al., 2012; Tarasova et al., 2018b). Table 1 shows a summary of developed method for identifying rainfall-runoff events. Rainfall-runoff event identification often involves separating baseflow, detecting rainfall and runoff events, and then pairing the corresponding rainfall events to runoff. In some cases, methods simultaneously detect and pair rainfall-runoff events (Giani et al., 2022). Rainfall-runoff event identification methods generally follow a pre-defined statistical framework, which relies on using parameters to specify rules to define individual events. Using statistical techniques with predefined parameters automates rainfall-runoff event identification which is beneficial when dealing with long records as well as large-scale analysis. For example, when detecting runoff events, a threshold parameter is typically used to filter out small runoff events in runoff event detection methods (Tang and Carey, 2017; Kaur et al., 2017). Or in some runoff event detection methods, a time interval parameter is used to ensure the independency of two consecutive peaks (Merz et al., 2006; Wasko and Guo, 2022). Pairing rainfall and runoff events also incorporates parameters. Pairing procedures are usually performed by applying a search window with the start of search, the search window length, and the searching direction (e.g., whether events are matched from runoff to rainfall or vice versa) all acting as parameters (Wasko and Guo, 2022). Selecting appropriate parameter values for rainfall-runoff event identification is complicated because of the absence of direct measurements for baseflow and quickflow (i.e. runoff). The lack of reliable "ground truth" data makes the choice of parameter value subjective, relying on expert judgment or site-specific calibration (Tang and Carey, 2017; Wasko and Guo, 2022). Although tracer studies can facilitate the estimation of baseflow values, they are expensive and not applicable for large scale analysis (Mei et al., 2024). Usually there are recommendations proposing a suitable range for parameter values (Nathan and McMahon, 1990), however, sensitivity analysis show that changes in the parameter value (i.e. "rules"), even in a valid parameter range, can significantly affect the rainfall-runoff events characteristics (Giani et al., 2022). For example, Wasko and Guo (2022) found that pairing from runoff to rainfall and vice versa, affects the selection of paired rainfall and runoff events, creating variability equal to that of the climatology due to biasing the runoff mechanism. Therefore, changing pairing rules affects characteristics of resulted rainfall-runoff events and significantly impacts the calculated catchment RCs. Current rainfall-runoff event identification methods usually use multiple parameters with no standard guideline on selecting parameter values resulting in large uncertainties in the events identified magnitudes (Mohammadpour Khoie et al., 2025). From here on in, we refer to the differing rainfall-runoff event identification due to differing parameter values as the "uncertainty" of rainfall-runoff identification.

For a single catchment, any given parameter value used for event identification may bias towards a limited range of event magnitudes (Mohammadpour Khoie et al., 2025). For example, selecting a larger threshold leads to detecting large runoff events only (Leenman et al., 2023). The limited representation of rainfall-runoff events over their full range of magnitudes prevents comprehensiveness in understanding catchment response. Appropriate parameter values vary across climatic regions, limiting transferability (Merz and Blöschl, 2009; Giani et al., 2022). For instance, when using a time parameter to separate independent runoff events, users may need to specify lower values for regions with shorter runoff events, and a purely statistical runoff event detection method may split a multi-peak runoff event into two independent runoff events under some settings. Runoff event detection and rainfall-runoff pairing are also usually performed as two separate steps, which increases the likelihood of mismatched events leading making unrealistic results, leading to rainfall-runoff events with RCs ≥ 1 which are physically implausible (Mohammadpour Khoie et al., 2025). Moreover, pairing is often conducted using a time-invariant search window, a simplification that does not reflect the underlying physical processes. To address the challenges in rainfall-runoff event identification, a transferable method that integrates conceptual understanding of rainfall-runoff processes with statistical techniques is needed. Such a method should provide consistent event detection across parameter choices and enable large-scale event-based streamflow analysis.

This study presents a novel, robust and transferable rainfall-runoff event identification method building on the runoff event definition proposed by Fischer et al. (2021). We extend the definition proposed Fischer et al. (2021) which

Table 1. A summary of literature of developed methods for identifying rainfall-runoff events.

Reference	Method description		Application area
	Runoff detection	Rainfall-runoff pairing	
Merz et al. (2006)	Runoff events identified on direct runoff using peak ratio.	Linear-reservoir model fitted to estimate runoff coefficient.	337 catchments in Austria
Metcalfe and Schmidt (2016)	Runoff events are detected based on peaks over a specific threshold. The difference between a peak and the neighboring valley is used to ensure about the independency.	–	–
Tang and Carey (2017)	Local minima values are recognized as valleys. The absolute difference between valleys is used to confirm termination of runoff events. The time difference between valleys is used to ensure independence of runoff events.	Pairing is optional using a backward search window.	1 catchment in Scotland, 1 catchment in the United Kingdom, and 1 catchment in Canada
Kaur et al. (2017)	Runoff events are detected based on the falling of baseflow index below a threshold.	–	Yarra River, Australia
Tarasova et al. (2018b)	Baseflow is first separated from total streamflow. Runoff events begin at the closest point before a flow peak where total streamflow equals baseflow and end when streamflow returns to the baseflow level; only events exceeding the specified peak threshold are retained.	Rainfall occurring with specific distance before the identified runoff event are considered as the contributing rainfall.	185 catchments in Germany
Fischer et al. (2021)	A variance-based method is used to detect sudden streamflow movements.	A search window is used to search backward from the start of detected runoff event.	7 catchments in Germany
Giani et al. (2022)	Detrending Moving-average Cross-correlation Analysis (DMCA) Detects runoff events based on rainfall events.		9 catchments in Great Britain

uses streamflow variance to detect sudden streamflow movements to pairing runoff events to rainfall in a parsimonious way. The novelty of our methods lies in (1) the method only relying on two parameters; (2) the method simultaneously detecting independent rainfall events and pairing them to runoff events, and (3) using a time-variant search window for pairing, which together improves robustness and transferability of rainfall-runoff event identification. We test the proposed rainfall-runoff event identification method against two benchmarking methods across catchments with diverse hydro-climate conditions. We show that the proposed rainfall-runoff event identification method maintains a low proportion of physically implausible RCs, while producing substantially lower uncertainty across parameter choices, indicating greater methodological robustness. Finally, we apply our proposed method across Australia to characterise rainfall-runoff processes across natural catchments.

2 Data

Here we use 467 Australian catchments which encompass a diverse set of hydrologic and climate conditions. These catchments were identified by the Australian Bureau of Meteorology's as Hydrologic Reference Stations (HRS) (Bureau of Meteorology, 2025a) as unregulated with minimal water resources development and land use change (Fig. 1). Located across the Australian continent the HRS catchments provide us with comprehensive data to compare rainfall-runoff rela-

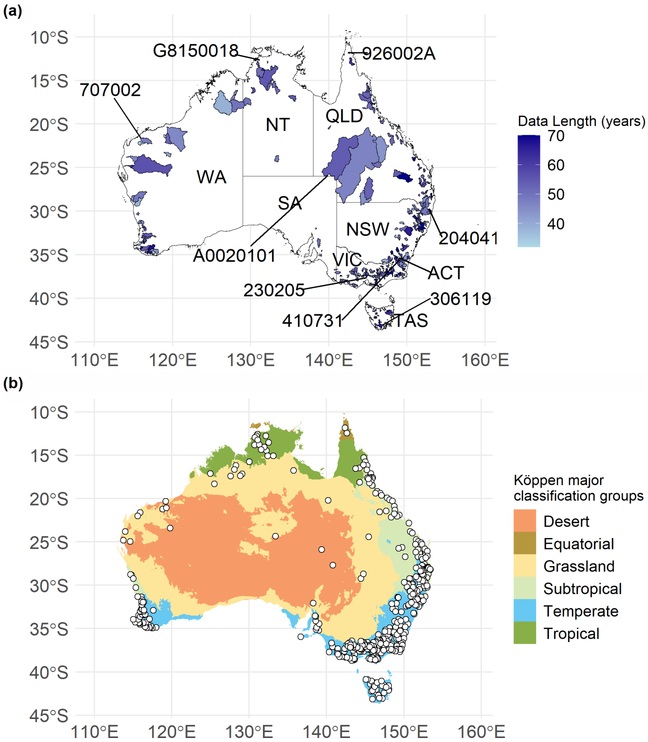

Figure 1. (a) Location and streamflow record length for the 467 HRS catchments over Australia within different states and territories (WA: Western Australia, NT: Northern Territory, QLD: Queensland, NSW: New South Wales, ACT: Australian Capital Territory, VIC: Victoria, TAS: Tasmania, SA: South Australia). **(b)** location of the 467 catchment outlets within various climates as defined by the Australian Köppen classification in (Stern et al., 2000). There are 7 sites in desert, 2 sites in equatorial, 23 sites in grassland, 58 sites in subtropical, 345 sites in temperate, and 32 sites in tropical regions. The 8 site IDs and arrows label the representative catchments selected across Australia for more detailed analyses.

tionships and test our proposed method for a wide range of hydro-climatic conditions. Daily recorded streamflow data at the outlet of each of the 467 catchments (in megalitre per day) were obtained for each of the HRS. The streamflow record at each station span at least 30 years extended through February 2024 (Bureau of Meteorology, 2025a). This dataset presents the highest quality long-term streamflow records in Australia which are widely used for large-sample hydrologic studies and assessing climate change-driven variability in streamflow (Wasko and Guo, 2022; Amirthanathan et al., 2023; Guo et al., 2020). Missing data accounts for less than 5 % and were infilled using GR4J model (Bureau of Meteorology, 2025a). Infilled flows make up $< 10\,\%$ of the total volume at each location, and $< 25\,\%$ of the total flow volume are flows produced using extrapolated rating curves (Bureau of Meteorology, 2025a). Here we divide the recorded streamflow by the catchment area to have units of $\mathrm{mm\,d^{-1}}$, consistent with the rainfall data.

Daily rainfall records (mm) were sourced from Australian Water Availability Project (AWAP), which provides a high-quality gridded rainfall product at a resolution of $0.05° \times 0.05°$ (approximately $5\,\mathrm{km} \times 5\,\mathrm{km}$) (Jones et al., 2009). AWAP has been extensively applied in Australian studies examining long-term, climate-driven trends (Jones et al., 2009) and is largely unbiased for calculating catchment average rainfall (Nathan et al., 2016; Nathan and McMahon, 2017; Wasko et al., 2023). Catchment averaged rainfall values were computed using the "AWAPer" R package (Peterson et al., 2020). In this study, rainfall represents the total accumulated precipitation (including rain, snow, hail, and dew) because rainfall dominates total precipitation in the study region, in line with the terminology used in the development of the AWAP (Jones et al., 2009).

From the 467 HRS catchments we selected 8 representative catchments across the continent to represent different climatic zones and geographic regions (represented by states). There are more selected catchments within the temperate climate zone because most HRS catchments are within this zone. The information for the selected catchments is presented in Table 2. The selected catchments are intended to spread across the continent as well as representing contrasting hydroclimatic and catchment-specific characteristics for testing the robustness of the proposed rainfall-runoff event identification methodology.

3 Methodology

3.1 The Robust Variance-based Event Identification Method (RVEIM)

We have named the proposed rainfall-runoff event identification method the Robust Variance-based Event Identification Method (RVEIM). RVEIM adopts the definition of runoff event from Fischer et al. (2021) who defined runoff event as "a temporally limited exceedance of normal discharges". Similar to Fischer et al. (2021), we used a moving window to estimate streamflow variance, which is used to identify sudden movement of streamflow. However, RVEIM adopts a different approach to detect runoff events beyond Fischer et al. (2021) by detection and pairing rainfall-runoff events while only using two parameters. Figure 2 present a flowchart of the developed method. Each major and minor step is explained in detailed in the following sections.

3.1.1 Streamflow statistics calculations

RVEIM detects runoff events when the streamflow time-series shows sudden short-term variation that clearly exceeds "normal" conditions. We defined "normal" conditions as the condition when baseflow is mostly contributing to streamflow (negligible runoff contribution). As such, prior to detecting runoff events and pairing them to corresponding rainfall, some statistics of the streamflow need to be calculated.

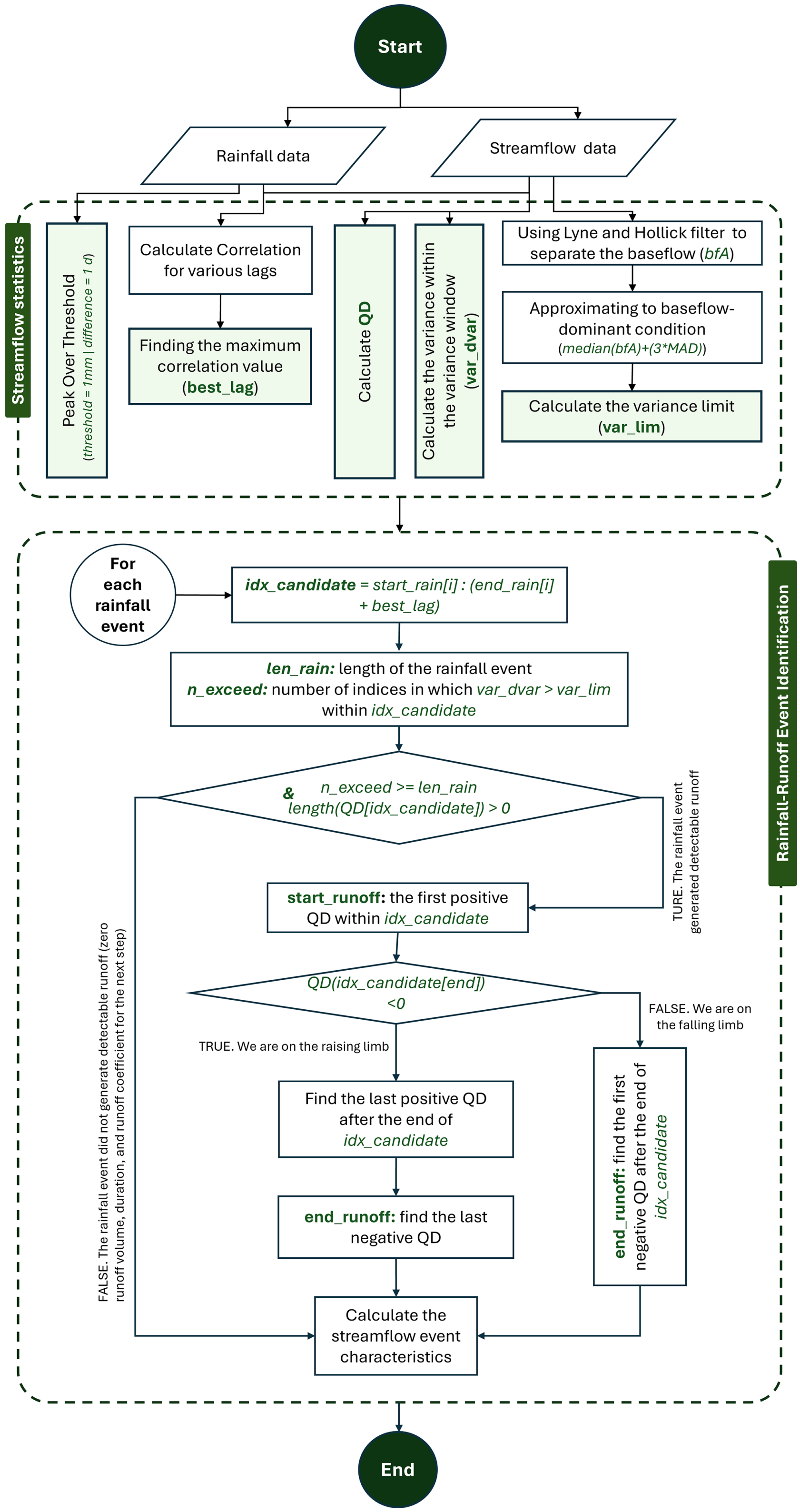

Figure 2. Flowchart of the RVEIM for identifying rainfall-runoff events.

Table 2. Hydroclimate and catchment-specific characteristics of selected catchments. Mean annual streamflow depth is expressed as an equivalent annual depth (mm), calculated by summing daily gauged flow in ML d^{-1} for each year, dividing by catchment area, and averaging across years.

State/ Territory	Station ID	Climate	Catchment area (km^2)	Mean annual temperature (°C)	Mean annual rainfall (mm)	Mean annual streamflow depth (mm)
SA	A0020101	Desert	11 9034.0	24.2	289.1	11.3
WA	707002	Grassland	7263.0	26.1	389.5	15.2
VIC	230205	Temperate	858.7	12.9	699.1	65.7
ACT	410731	Temperate	671.6	9.9	869.9	89.4
NSW	204041	Subtropic	1807.0	18.3	1366.2	432.7
TAS	306119	Temperate	1824.0	9.2	1625.0	1441.8
QLD	926002A	Equatorial	333.3	26.5	1628.0	690.6
NT	G8150018	Tropical	95.6	27.5	1637.4	652.8

These RVEIM statistics include calculating the moving variance, streamflow gradient, variance threshold of streamflow, and cross-correlation between rainfall and streamflow. The first three statistics are needed for runoff event detection, and the last is necessary for the subsequent rainfall-runoff event pairing.

1. *Moving variance window.* A moving variance window is employed to estimate the short-term variance of streamflow over time (Fischer et al., 2021). By doing so, it captures temporal fluctuations in streamflow variance, providing a dynamic assessment of variability. The length of the moving variance window is controlled by the parameter *d_var* (as the first parameter of RVEIM) which determines the number of observations included in each calculation.

2. *Streamflow gradient.* (QD) plays a role in defining the start and the end of runoff events. Therefore, before runoff event detection and pairing, the QD is needed to be calculated by simply subtracting the streamflow in the current time step from the previous time step as shown in Eq. (1).

$$\mathrm{QD}_i = Q_i - Q_{i-1}(1) \quad (1)$$

where Q indicates on daily streamflow value, and i and $i-1$ indicate on the current and the previous timesteps. Note that QD_1 cannot be defined as there is no streamflow record before the first time-step.

3. *Cross-Correlation*. A runoff event is paired to the corresponding rainfall event based on a time-varying search window controlled by two parameters (as shown in Eq. 2). The first parameter, which is constant across rainfall events, is *best_lag*. This parameter is defined as the lag between rainfall and streamflow that maximizes the cross-correlation between these variables (and is calculated prior to rainfall event detection). Physically, *best_lag* represents the average response time between rainfall and runoff. The second parameter controlling the length of the search window is *l_rainfall*, which corresponds to the duration of the rainfall event. Therefore, this parameter varies from one rainfall event to another.

$$length(search\_window_j) = best\_lag + l\_rainfall_j \quad (2)$$

where j is the counter of rainfall events and *l_rainfall* is the length of rainfall event.

4. *Variance threshold.* We defined a threshold for moving variance (*var_lim*), to consider any short-term variance of streamflow below as "normal" streamflow (i.e. exceedance as a runoff event). We propose an approach that is easily transferable to other catchments. To find the variance of baseflow-dominated condition, we firstly used the Lyne and Hollick (1979) baseflow filter to extract the baseflow timeseries from the total streamflow timeseries. This baseflow filter is widely used in the literature (Wasko and Guo, 2022) and has a filter parameter (*alpha* – the second parameter of RVEIM). Since baseflow increases during a runoff event, the separated baseflow should be processed to identify the non-event portion of baseflow. To exclude event-influenced high-flow, we removed baseflow that are larger than *limit* which was estimated as the upper bound of baseflow under normal conditions. Specifically, the Median Absolute Deviation (MAD) of baseflow (Eqs. 3 and 4) was used:

$$\mathrm{MAD} = median(abs(baseflow - median(baseflow)) \quad (3)$$

$$limit = median\,(baseflow) + 3 \cdot \mathrm{MAD} \quad (4)$$

Then, the variance of baseflow values below limit is considered as the threshold below which the local variance of streamflow is considered as "normal" flow

(Eq. 5).

$$var\_lim = variance(baseflow < limit) \tag{5}$$

Although this process in Eqs. (3) and (4) is known as "outlier" removal (Voloh et al., 2020), we use it for approximating the baseflow-dominant condition. The multiplier of 3 (in Eq. 4) was adopted because this threshold is commonly used in outlier detection procedures. The variance of baseflow values below *limit*, which we considered as representative of baseflow-dominated condition, is considered as the threshold. Figure 3 shows the process of obtaining *limit* for catchment "230205" in the temperate region from the streamflow timeseries.

3.1.2 Runoff event detection and pairing

Runoff event detection and pairing start after detecting rainfall events. We apply the widely used Peak Over Threshold (POT) approach for detecting independent rainfall events. Two parameters are associated in POT including the threshold above which a rainfall amount is meaningful and the minimum time difference between two successive events (Wasko and Guo, 2022). Numerous studies have confirmed that POT with 1 mm threshold and 1 d minimum difference is appropriate to identify rainfall events with daily data (Ashcroft et al., 2019; Wasko and Guo, 2022; Zhang et al., 2011). In contrast to most rainfall-runoff event identification methods, RVEIM detects and pairs runoff events simultaneously. For each rainfall event, a search window is specified to search for a probable corresponding runoff event. The search window is the summation of *best_lag* and the length of rainfall *l_rainfall* (i.e., *best_lag* $+$ *l_rainfall* as mentioned in Eq. 2) and starts from the beginning of the rainfall event (see dashed vertical lines in Fig. 4). After defining the length of the search window, for the current rainfall event, the method searches for any sign of streamflow movement. So, unlike most pairing strategies, the strategy here does not search for the peak of the runoff event within the search window. In the search window, if the length of streamflow records which exceed *var_lim* is greater or equal to the length of rainfall, the first positive QD represents the start of the runoff event (see the start of bold line of streamflow for both events in Fig. 4). Otherwise, there is no runoff event in the search window. This condition reflects the expectation that a rainfall event leading to runoff should produce a sufficiently sustained streamflow response, rather than a short-lived or spurious fluctuation which might be due to instrumental errors. For any rainfall event, if the search window overlaps with a previously detected and paired runoff event, the start of the search window is modified to the end of the runoff event without any modification of the end of the search window (compare shaded area and dashed vertical lines in second runoff event in Fig. 4). To specify the end of the runoff event, the last streamflow record of the search window should be checked. If the QD of the last streamflow record is negative (first runoff event in Fig. 4), the RVEIM moves forward to find the last negative QD (it assumes being on the falling limb, so continues to find the end of falling limb). Otherwise (see the second runoff event in Fig. 4), it continues to find the peak and then the last negative QD. After finding the start and the end of the runoff event, the volume of runoff is calculated by subtracting the volume of baseflow from streamflow in the event duration.

3.2 Benchmarking the rainfall-runoff event identification

To demonstrate the advantages of the RVEIM, we compare our results with existing methods. Since there are numerous rainfall-runoff event identification methods we benchmark RVEIM against two complementary methods. First, we implemented a commonly used method which uses local maxima to identify events before pairing the streamflow to the driving rainfall (Wasko and Guo, 2022). Following the recommendation by Mohammadpour Khoie et al. (2025) which compared event identification methods, the local maxima method generally had less uncertainty in its outputs; and as such, we included the local maxima as one benchmark method. Second, the Detrending Moving-average Cross-correlation Analysis (DMCA) method developed by Giani et al. (2022) is included as its methodological complexity is closer to that of RVEIM, providing a more comparable benchmark for assessing the performance and transferability of the proposed method.

To detect runoff events, the local maxima method firstly detects local maximum values in streamflow/runoff timeseries. Then, by comparing each peak with the next valley it decides about a new runoff event: if the difference between a peak with the next valley is higher than a user-defined value (*delta.y*), a new runoff event is detected. Otherwise, the peak is part of a multi-peak runoff event. To filter out small runoff, the local maxima method considers a minimum *threshold* above which runoff is considered. A minimum spacing between two consecutive runoff events (*delta.x*) is considered to ensure independency of runoff events.

DMCA identifies rainfall-runoff events by analysing rainfall and streamflow time series simultaneously. The method estimates a characteristic catchment response time and uses it to detect event cores where rainfall and streamflow fluctuations are jointly active. Event boundaries are then refined using the behaviour of the individual rainfall and streamflow fluctuations, with a rainfall fluctuation tolerance used to prevent negligible rainfall from merging otherwise separate events. This allows DMCA to define events as coupled rainfall-runoff system realizations.

Baseflow separation is handled differently across the three event identification methods used in this study and may be applied either before or after runoff event detection. In the local maxima method, baseflow is usually separated before

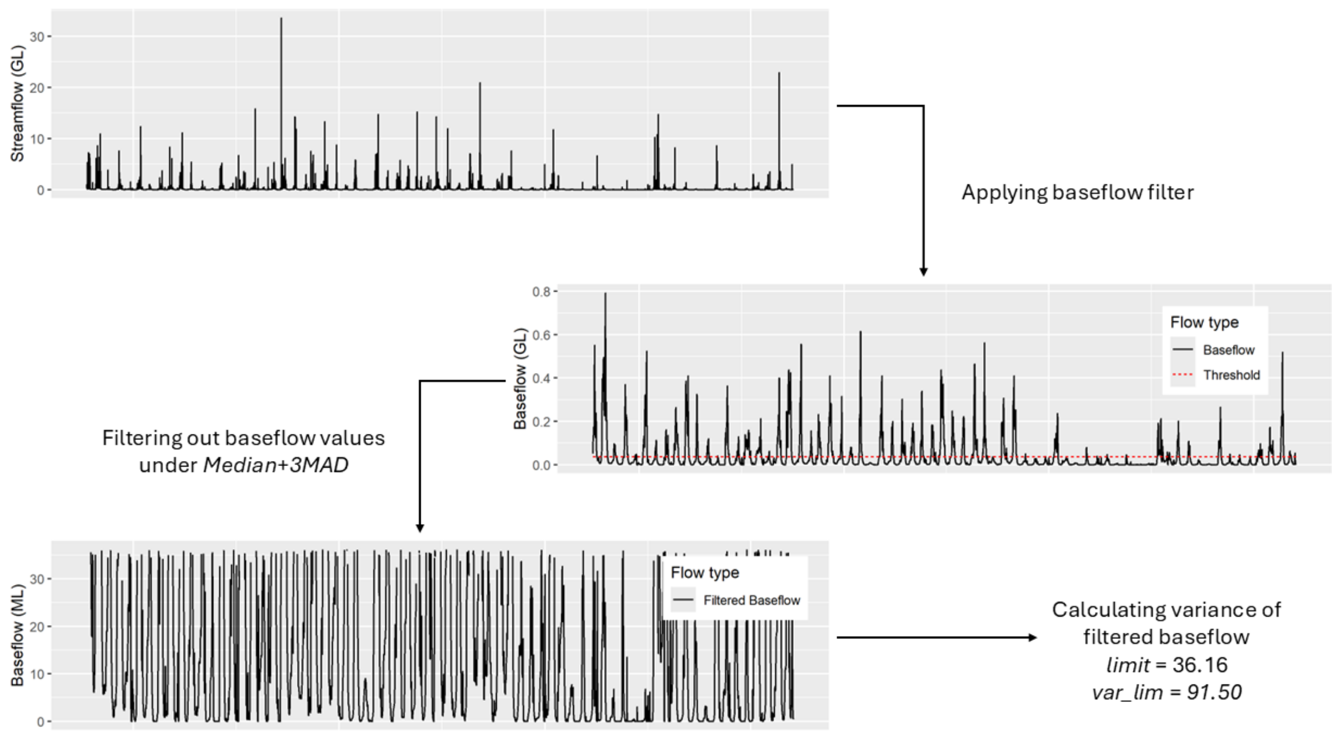

Figure 3. The process of obtaining the *var_lim*.

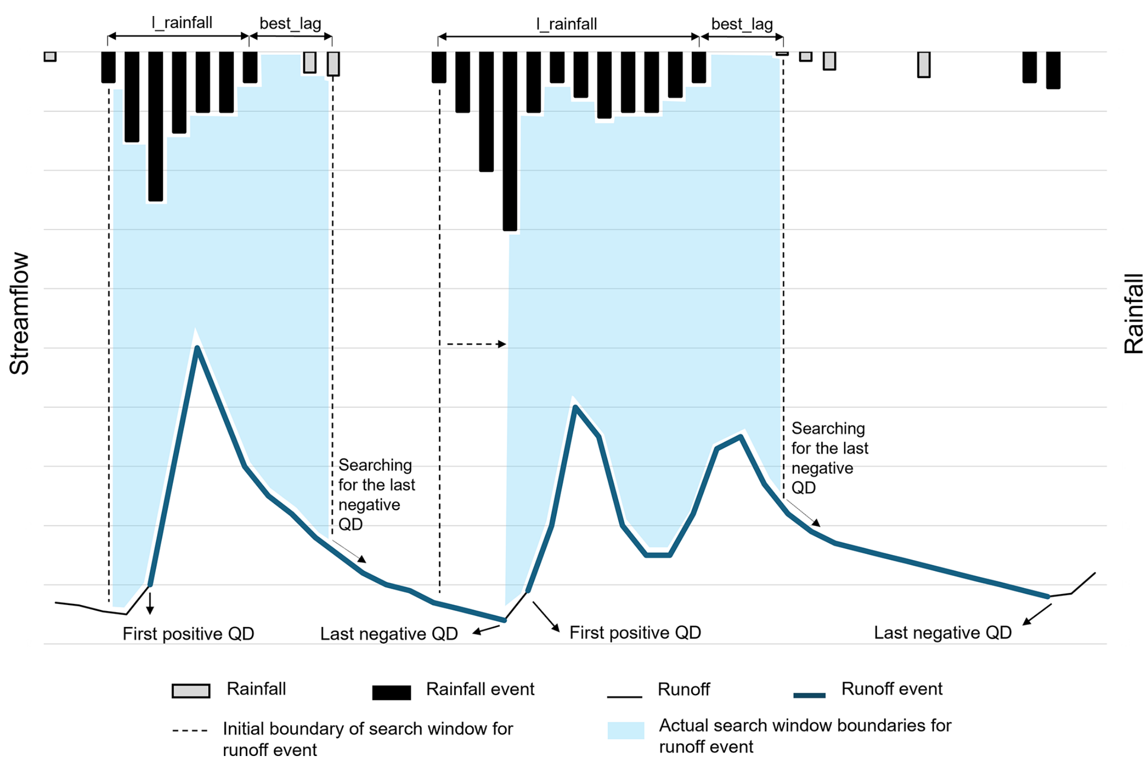

Figure 4. Schematic of the runoff event detection and pairing procedure.

runoff event detection so that runoff events are identified from quickflow (the part of streamflow which directly comes from rainfall). However, in RVEIM and DMCA, the baseflow volume is subtracted after detecting the runoff event. Further, DMCA estimate the baseflow by connecting the streamflow values at the beginning and the end of each detected runoff event (Giani et al., 2022) while RVEIM and local maxima use a digital baseflow filter (as described in Sect. 3.1.1 and 3.1.2). The Lyne and Hollick (1979) baseflow filter which is widely used in the literature (Wasko and Guo, 2022; Ladson et al., 2013; Kemp and Alankarage, 2023; Miao et al., 2020; Ho et al., 2022) was used in this study. The filter separates baseflow with the help of a parameter called the "filter parameter". The filter parameter varies between 0 and 1 and defines how the digital filter should respond to streamflow variation. Lower values of the filter parameter indicate on a quicker response to streamflow changes. Nathan and McMahon (1990) investigated the best choice of filter parameter. They showed the range of 0.9–0.95 for filter parameter works better and recommended the value of 0.925 for better performance of the filter.

The pairing process differs slightly among the methods used: RVEIM and DMCA identify rainfall-runoff event pairs jointly, whereas local maxima detects rainfall and runoff events separately and pairs them afterwards. In local maxima, the pairing uses a search window to pair each rainfall to a corresponding runoff event. Five pairing strategies are included in local maxima which are different in their directions and start points used for searching. Pairing type 1 searches from the start of rainfall event to the peak of runoff event. Pairing type 2 searches from the start of rainfall event to the end of runoff event. Pairing type 3 searches from the peak of runoff event to the peak of rainfall event. Pairing type 4 searches from the start of runoff event to the start of rainfall event. Pairing type 5 searches from the peak of rainfall event for the peak of runoff event both forwards and backwards. The pairing type and length of search window (*lag*) are both user-specified.

3.3 Evaluation

To assess the uncertainty associated with parameter value selection in all methods, a sensitivity analysis is performed for the sites representing different climates and regions listed in Table 2. A plausible range is specified for each parameter for each rainfall-runoff event identification method. Then, random samples within the parameter range are drawn and used for identifying rainfall-runoff events. The changes in characteristics of rainfall-runoff events are then analyzed to understand the uncertainty in rainfall-runoff event detection due to parameter change. The characteristics here are the mean annual number, volume, length, and RCs of paired runoff events (i.e., runoff events matched to rainfall events and having runoff volumes greater than zero). This combination of characteristics was selected to determine which method yields acceptable variability in the identified event characteristics while maintaining an acceptable level of physical plausibility. We estimate the ECDF of RCs for each sampled parameter set and then across each catchment considering the 95 % confidence interval (between 2.5th percentile and 97.5th percentile) as it reveals how each method represents the characteristics of individual catchment across the full distribution of RCs.

Two parameters are associated with the development of RVEIM: the length of the moving variance window, *d_var* (Sect. 3.1.1) and the filter parameter of the baseflow digital filter, *alpha*. For the benchmarking methods, local maxima event identification method uses six parameters: *alpha* for rainfall event detection, *Threshold*, *delta.x*, *delta.y* for runoff event detection, and *type* and *lag* for pairing rainfall and runoff events, and DMCA uses two parameters: *rain_min*, which is the minimum rainfall intensity threshold, and *max_window*, which is the maximum search window for estimating the catchment response time.

The parameter ranges adopted for the three rainfall-runoff event identification methods were selected based on previous studies and the methodological characteristics of each approach. Therefore, for the local maxima method, the parameter ranges were adopted from Mohammadpour Khoie et al. (2025) based on the dynamics of streamflow in different climate zones. For DMCA, the ranges for the *rain_min* and the *max_window* were derived from the example implementation provided with the original method (Giani et al., 2022). For RVEIM, the alpha range is considered between 0.9 and 0.95 as recommended by Lyne and Hollick (1979). To specify a plausible range for the length of moving variance window (Sect. 3.1.1) we used the range of 3–10 d. The maximum 10 d was chosen to capture the temporal variability of runoff events without excessively smoothing the data. This range was informed by the range specified by Fischer et al. (2021) which proposed another variance-based runoff event detection method. We generated 300 random samples (i.e., parameter sets) for RVEIM and DMCA and 600 samples for local maxima to properly cover the parameter space for each method.

Rainfall event detection is considered a deterministic process in RVEIM and local maxima methods meaning uncertainty is not investigated. Here, the POT method with 1 mm threshold is appropriate to identify rainfall events (Ashcroft et al., 2019; Wasko and Guo, 2022; Zhang et al., 2011).

4 Results

The results are presented in multiple parts. We firstly present detailed time-series of identified rainfall-runoff events for a single catchment to demonstrate the application of RVEIM (Sect. 4.1). Then, we compare the uncertainty and reliability of the RVEIM with the benchmarking methods for 8 representative catchments with diverse climatic conditions

(Sect. 4.2). Finally, the variation of rainfall-runoff relationship across Australia derived using the RVEIM are investigated across various climates (Sect. 4.3).

4.1 Demonstrating rainfall-runoff event identification for a single catchment

To demonstrate the performance of the proposed rainfall-runoff event identification method, we chose catchment 306119 in Tasmania. Within the eight representative catchments, 306119 has the third highest annual rainfall and the largest annual streamflow (Table 2). As one of the wetter catchments, identifying rainfall-runoff events is more challenging as there are a higher number of rainfall-runoff events and usually a higher baseflow contribution to streamflow through year which makes it harder for statistical rainfall-runoff event identification methods to identify events precisely. Consequently, adequate performance of a rainfall-runoff event identification method in such a catchment means it will likely obtain satisfactory performance in other catchments. Here an example event identification with RVEIM with *alpha* 0.904 and *d_var* 3 (one random sample of the 300 random parameter sample sets drawn, as detailed in Sect. 3.3) is presented. Figure 5 shows identified rainfall-runoff events from 1 June 1973 to 1 September 1973, with each pair of identified rainfall and runoff events highlighted in the same color on top of the original time-series in black. Within the selected period, 11 rainfall events are recognized with 8 runoff events detected and paired with rainfall. Although some rainfall events have suitable volume for generating runoff, they did not lead to runoff events because the variance does not exceed the *var_lim* (Sect. 3.1). Both small and large runoff events including single-peak and multi-peak runoff events are detected and paired demonstrating the power and flexibility of RVEIM. Some streamflow peaks (for example, the small peak after the first runoff event toward mid-June) are not detected since the variance is lower than *var_lim*. Note that such events have minor effects on streamflow analysis even if they are detected and paired, and the key point demonstrated here is that the pairing appears plausible and consistent with our physical understanding.

Although the same runoff event identification rules are applied consistently to all events, some events may appear visually truncated, such as the third and fourth runoff events in Fig. 5 (shown in green). This mainly reflects the temporal discretization involved in delineating runoff events from daily data. Shifting the runoff event start one time step earlier could make the runoff events appear more visually complete, but it produces only negligible changes in event characteristics and may incorrectly double-count time steps by creating overlap between the beginning of one runoff event and the end of the preceding event.

Table 3. Ranges considered for parameters in each method for selected catchments. Terms denoted by italics represent variables defined in the method (e.g. limit in Eq. 4), rather than ordinary words.

Station ID			A0020101	707002	230205	410731	204041	306119	926002A	G8150018
RVEIM	*alpha*	–	0.9 to 0.95	0.9 to 0.95	0.9 to 0.95	0.9 to 0.95	0.9 to 0.95	0.9 to 0.95	0.9 to 0.95	0.9 to 0.95
	d_var	*(d)*	3 to 10	3 to 10	3 to 10	3 to 10	3 to 10	3 to 10	3 to 10	3 to 10
Local maxima	*alpha*	–	0.9 to 0.95	0.9 to 0.95	0.9 to 0.95	0.9 to 0.95	0.9 to 0.95	0.9 to 0.95	0.9 to 0.95	0.9 to 0.95
	threshold	(ML)	0 to 5	0 to 5	0 to 250	0 to 250	0 to 5	0 to 250	0 to 250	0 to 250
	delta.y	–	−0.9 to −0.7	−0.9 to −0.7	−0.9 to −0.7	−0.9 to −0.7	−0.9 to −0.7	−0.9 to −0.7	−0.9 to −0.7	−0.9 to −0.7
	delta.x	(d)	1 to 10	1 to 10	1 to 10	1 to 10	1 to 10	1 to 10	1 to 10	1 to 10
	type	–	1 to 5	1 to 5	1 to 5	1 to 5	1 to 5	1 to 5	1 to 5	1 to 5
	lag	(d)	1 to 7	1 to 7	1 to 7	1 to 7	1 to 7	1 to 7	1 to 7	1 to 7
DMCA	*rain_min*	($mm\,d^{-1}$)	0.02 to 100	0.02 to 100	0.02 to 100	0.02 to 100	0.02 to 100	0.02 to 100	0.02 to 100	0.02 to 100
	max_window	*(d)*	50 to 100	50 to 100	50 to 100	50 to 100	50 to 100	50 to 100	50 to 100	50 to 100

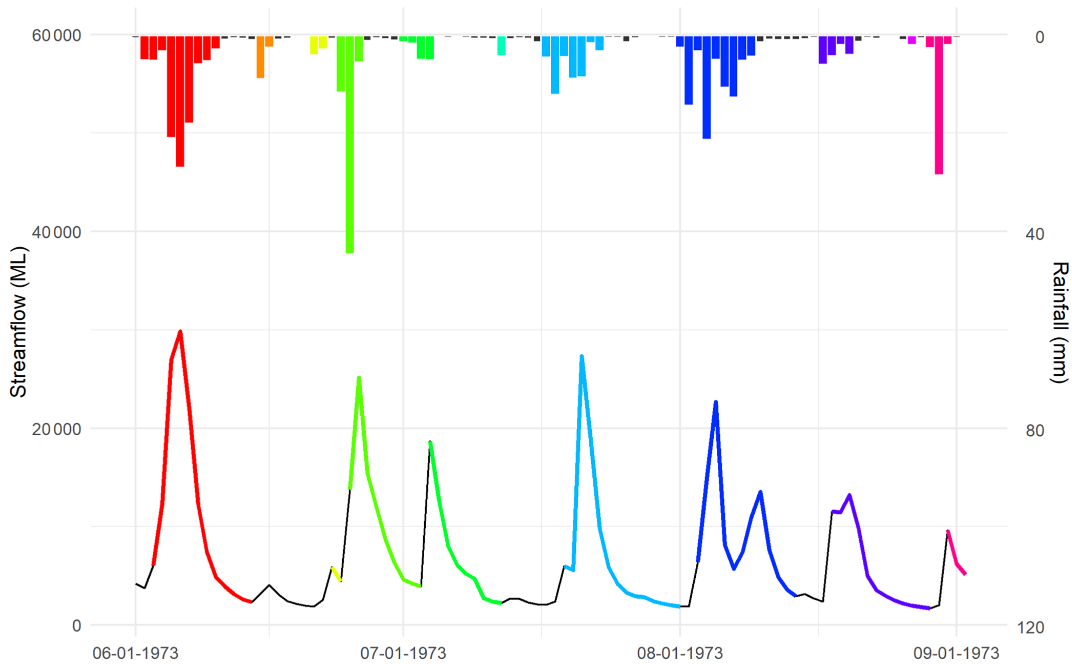

Figure 5. Identified rainfall-runoff events from 1 June 1973 to 1 September 1973 in catchment 306119. Rainfall is shown as a reversed barchart and streamflow is shown as a line. Each pair of identified rainfall and runoff events is highlighted in the same color on top of the original time-series.

4.2 Comparing the RVEIM with benchmarking methods

Mean annual characteristics of paired runoff events are extracted from all three methods over all samples. Figure 6 demonstrates that local maxima generally exhibits the greatest uncertainty in the characteristics of the identified paired runoff events, whereas RVEIM consistently produces lower uncertainty across the representative catchments, highlighting the higher robustness of the proposed method against parameter value change. The uncertainty of RVEIM and DMCA are similar to each other for most cases, but RVEIM generates lower uncertainty for some sites and event characteristics (for example, the mean volume of paired runoff events in Fig. 6c). The uncertainty associated with DMCA varies depending on both the considered characteristic and the catchment. For example, DMCA shows markedly higher uncertainty in the mean length of paired runoff events for the desert catchment A0020101 than for the other catchments (Fig. 6b), suggesting that its performance may vary considerably under certain climatic conditions. Boxplots of paired runoff event characteristics detected by the local maxima method includes many outliers, with much fewer when using the RVEIM. Noticeably there are fewer outliers in the average annual number rainfall-runoff events identified by RVEIM (Fig. 6a) providing more confidence on number of paired runoff events. Considering the mean length and volume of paired runoff events (Fig. 6b and c), it can be concluded that local maxima generally finds shorter but larger runoff events meaning local maxima probably biases towards large runoff events while RVEIM and DMCA perform better in identifying a broader range of runoff events.

Assuming the measured rainfall and runoff are accurate, errors in rainfall-runoff event identification can come from detecting the start and end of rainfall and runoff events, and pairing runoff events to rainfall, which lead to uncertainties in estimating the runoff events' volume. Here, to examine the reliability of implemented methods, we compare the percentage of RCs > 1. A higher percentage of RCs > 1 means there are more physically implausible rainfall-runoff events and hence a lower reliability in the identified events.

Figure 7 shows the percentage of RCs > 1 for rainfall-runoff events identified by the three methods for the 8 representative catchments. Each boxplot presents the variability of percentage of RCs > 1 over the full sample of parameter sets. The percentage of RCs > 1 is generally lowest for DMCA, while RVEIM also produces substantially lower percentage of RCs > 1 than local maxima across most catchments. All catchments identified by DMCA and RVEIM show very low percentage of RCs > 1 (except for catchment 306119 – below 4 % for RVEIM and 0 % for DMCA) with limited sensitivity to parameter values change (shown by the interquartile range of the boxplot). However, the percentage of RCs > 1 in local maxima is consistently higher and vary across a wider range for all catchments with changing parameter values. Among all catchments, the three wettest catchments (306119, 926002A and G8150018) have both higher percent-

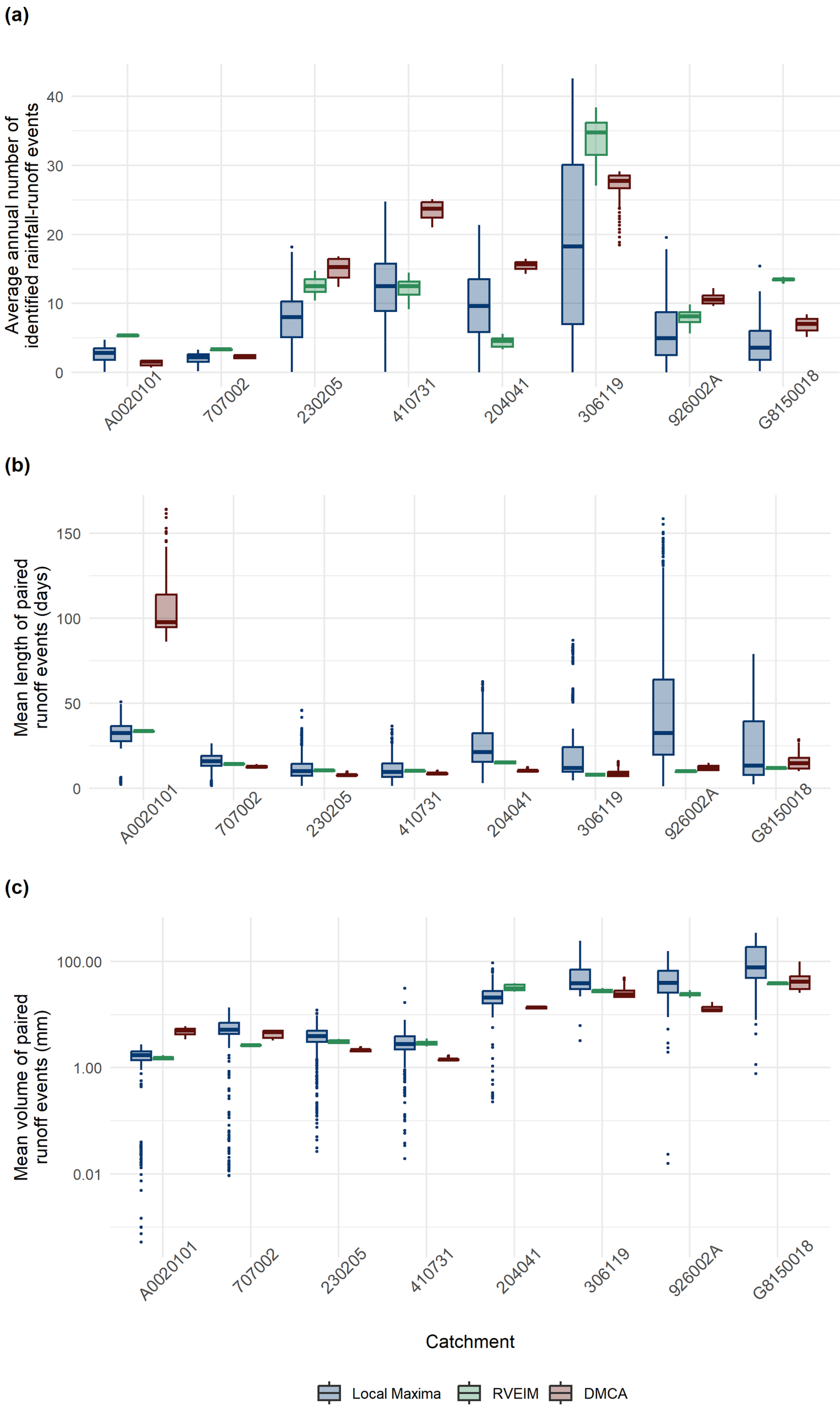

Figure 6. Boxplots of annual characteristics of paired runoff events identified by the implemented methods. **(a)** average annual number of rainfall-runoff events. **(b)** mean length of paired runoff events **(c)** mean volume of paired runoff events (log-scale). The outliers in each panel are identified with the first quartile (Q1), third quartile (Q3) and interquartile range (IQR), as points lower than (Q1) – $1.5 \cdot \mathrm{IQR}$ or higher than (Q3) + $1.5 \cdot \mathrm{IQR}$.

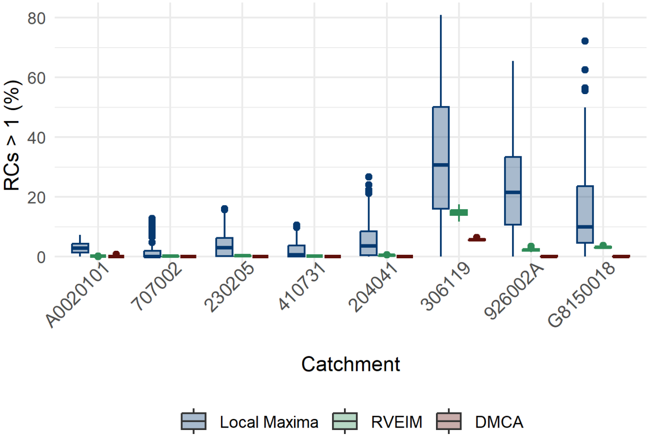

Figure 7. Percentage of RCs > 1 across representative catchments.

ages and variability of RCs > 1 in all methods (especially, local maxima). This highlights the challenge for rainfall-runoff event identification in wetter catchments, which is further discussed in Sect. 5.

As a signature of catchment response, the Empirical Cumulative Distribution Function (ECDF) of RCs informs the event-scale rainfall-runoff relationship. Here we compare the uncertainties in the ECDFs of RCs obtained using the implemented methods, over all parameter samples used (Fig. 8). Since rainfall-runoff events with RCs > 1 are physically implausible, we have estimated the ECDFs of RCs with rainfall-runoff events with $0 < \text{RCs} \leq 1$. As demonstrated in Fig. 7, with the RVEIM there is generally only a small number of identified events with RCs > 1 (less than 4 % for most catchments), therefore omitting rainfall-runoff events with RCs > 1 is not expected to greatly impact the ECDF of RCs for an individual catchment.

The RVEIM and DMCA have a significantly narrower uncertainty band in the ECDFs compared to using local maxima for event identification across all representative catchments. For example, the probability of identifying a rainfall-runoff event with RC < 0.25 in catchment 926002A is roughly between 0.3–1 when the local maxima method is used (Fig. 8g). However, the probability of identifying rainfall-runoff events with RC < 0.25 is approximately 0.48–0.65 when the RVEIM is used and approximately 0.96–0.98 when DMCA is used, indicating greater confidence. The uncertainty in the ECDF of RCs varies considerably between catchments among all methods. For example, the uncertainty in catchment A0020101 is much lower than catchment 306119 for all methods (Fig. 8a and f). The change of uncertainty across catchments is likely due to differing catchment responses and climatic conditions. Rainfall-runoff events are identified with greater certainty for drier catchments, where there are fewer number of rainfall/runoff events and a steady contribution of baseflow throughout a year (e.g. catchment A0020101 in Fig. 8a).

The shape of the ECDF of RCs contains important information regarding the rainfall-runoff events in a catchment. A steeper ECDF emphasizes that there is a mass of rainfall-runoff events with a limited range of RCs. A more gradually increasing ECDF represents a wider range of RCs with a more uniform distribution. For example, in catchment A0020101 (Fig. 8a), there is a sharp increase in the slope of the ECDFs between $\text{RC} \approx 0$ and approximately 0.125, reaching around 70th percentile, meaning that all methods agree that most rainfall-runoff events (around 70 % of rainfall-runoff events) have the RC between 0-0.125. However, in catchment G8150018 (Fig. 8h), the ECDF increases smoothly between $\text{RC} \approx 0$ to 0.25 up to around 50th percentile meaning a more uniform distribution of rainfall-runoff events with RCs between 0 and 0.25.

The median of ECDFs for all methods are quite close for some catchments, like catchment 707002 (Fig. 8b). However, in some catchments, like catchment 204041 or 926002A (Fig. 8e and g), there is a meaningful separation between methods. The separation among the methods indicates the contrasting representation of the catchment behavior. For example, in catchment 926002A, for low RCs, the median of local maxima method increases relatively gradually, suggesting that identified rainfall-runoff events are distributed relatively evenly across this range (approximately 17 % of rainfall-runoff events have RCs < 0.05 – Fig. 8g). In contrast, the median of DMCA rises sharply near zero, indicating a greater concentration of rainfall-runoff events with zero or very low RCs (around 69 % of rainfall-runoff events have RCs < 0.05). The median of RVEIM remains considerably below the other two curves over much of the low-RC range, indicating fewer rainfall-runoff events with near-zero RCs (only around 3 % of rainfall-runoff events have RCs < 0.05). Consequently, RVEIM physically represents this catchment as having a greater potential to convert event rainfall into runoff. Given that catchment 926002A is Equatorial in climate and relatively wet (the second highest mean annual rainfall and streamflow according to Table 2), the event representation by RVEIM is likely more hydrologically plausible. This disagreement between methods is also evident in catchment 204041 (Fig. 8e). In catchment 204041, DMCA shows around 69 %, local maxima shows around 26 %, and RVEIM suggests only 2 % of rainfall-runoff events with $\text{RCs} \leq 0.05$. As shown in Fig. 8, the disagreement between methods are more pronounced when moving towards wetter catchments (i.e. catchments presented in later panels, as they are ordered by annual rainfall as per Table 2), where RVEIM consistently indicates a greater potential for runoff generation, which appears hydrologically plausible. Considering the demonstrated robustness and reliability of RVEIM in producing more realistic rainfall-runoff event behavior, the subsequent sections focus only on results generated from RVEIM.

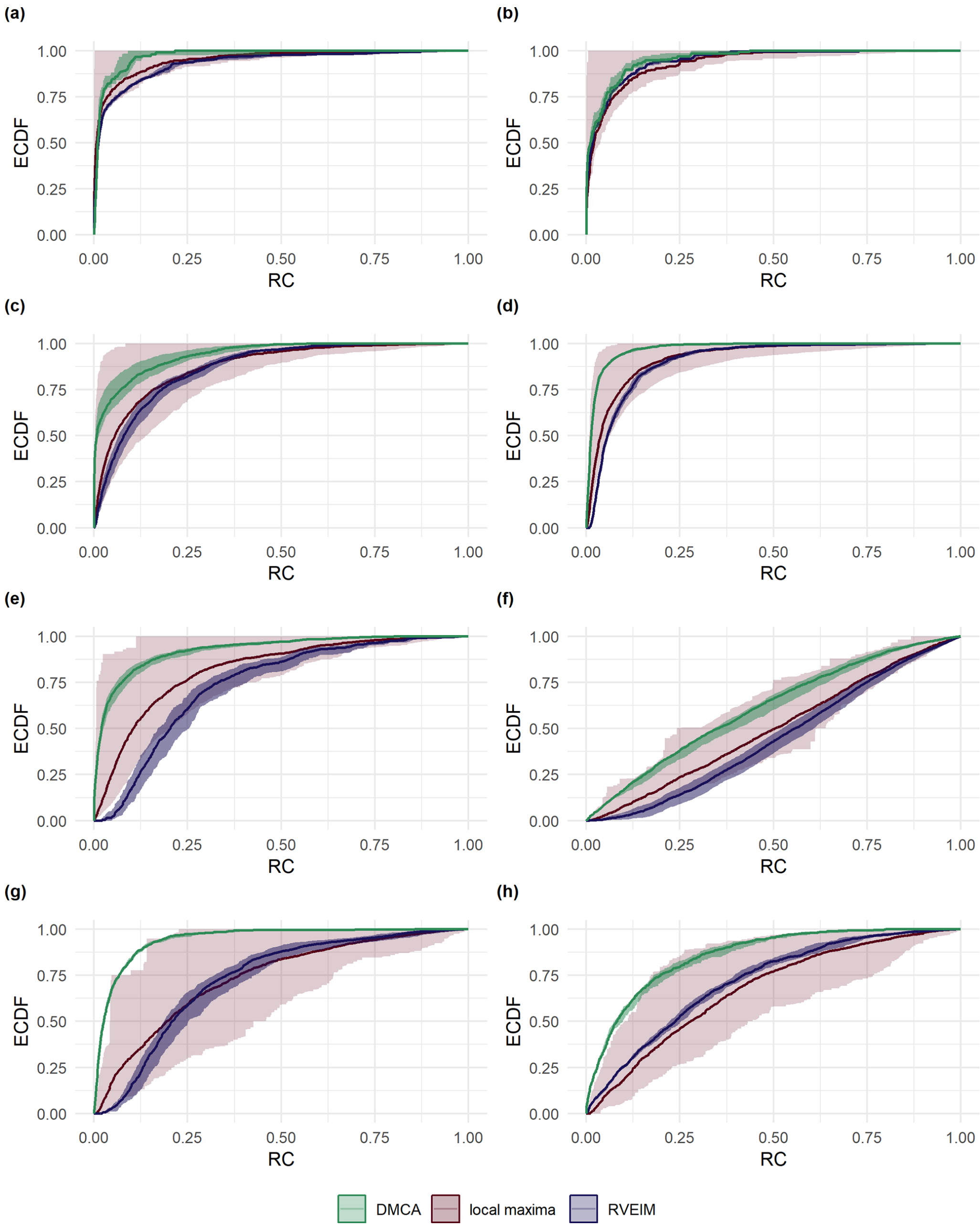

Figure 8. The ECDF of RCs using the implemented methods (rainfall-runoff events with RCs > 1 are omitted **(a)** catchment A0020101. **(b)** atchment 707002 **(c)** catchment 230205 **(d)** catchment 410731. **(e)** catchment 204041. **(f)** catchment 306119. **(g)** catchment 926002A. **(h)** catchment G8150018. In all panels, the 95 % uncertainty band and the median across samples for each rainfall-runoff event identification method are shown in shades and a continuous line, respectively.

4.3 Characterising Australian catchment responses

The RVEIM is applied to all 467 HRS catchments in Australia. The characteristics of rainfall and runoff events are extracted and the mean value over 300 parameter samples are plotted in Fig. 9. There is a clear increase of the average annual number of rainfall events from northwestern to south-eastern Australia (Fig. 9a). There is a positive correlation between the average annual number of rainfall and runoff events except for catchments in the north and south-west of Australia. For these regions, although the average annual number of rainfall events is lower (Fig. 9a), the average annual number of runoff events is similar to other catchments in southern Australia (Fig. 9b). A positive correlation between mean length of rainfall and runoff events is also seen except for western Tasmania (see Fig. A1 in Appendix A). Although catchments in western Tasmania have longer rainfall events than other catchments (Fig. 9c), their corresponding runoff events are shorter compared to other catchments (Fig. 9d). The shorter duration of runoff events in Tasmania can be explained by the steeper slopes of catchments in Tasmania which develop quick flow paths (Douinot et al., 2022). A high positive correlation between the mean volume of runoff and rainfall events is also detected (Fig. A2) with some inconsistencies for catchments in northern WA. Catchments in northern WA have the lowest mean volume of rainfall (Fig. 9e), however they have relatively larger mean annual volume of runoff (Fig. 9f) pointing to lower losses in these catchments compared to others. This can be explained by the relatively lower evapotranspiration (Fig. A3) and higher soil moisture (Fig. A4) in northern WA (Bureau of Meteorology, 2025b, c) meaning lower rainfall losses and higher potential of runoff generation. Figure 9g presents mean RC values of identified rainfall-runoff events across Australia. Higher RC values are concentrated around coasts pointing out that catchments around coasts have higher potential of runoff generation. Among all catchments, catchments in Tasmania obtained highest RCs which can be a combined effect of the lower evapotranspiration and significantly higher soil moisture in Tasmania (Bureau of Meteorology, 2025c, b). The percentage of RCs > 1 within all events identified for each catchment is shown in Fig. 9h. The mean percentage of RCs > 1 is below 6 % for almost all catchments (around 90 % of catchments). However, the ~ 10 % of catchments that have 6 %–25 % of RCs > 1 are mostly concentrated in the east of Australia and Tasmania. Catchments in east coast of Australia and Tasmania which generally have higher soil moisture (highest in Tasmania). Higher soil moisture increases the runoff volume and the RC as well (Song and Wang, 2019; Schoener and Stone, 2019). The increase in RC, on the other hand, increases the potential of estimating RCs > 1 because of errors in runoff volume estimation (Mohammadpour Khoie et al., 2025). The potential errors leading to RCs > 1 are further discussed in Sect. 5.2.

Figure 10 compares the ECDF of RCs in each climate region by presenting the median of ECDFs of RCs across the 300 parameter samples of individual catchments within each climate region. This provides the first Australia-wide summary of the distribution of event RCs. Where the ECDF of RCs has a sharp increase at the beginning it means that there is a mass of rainfall-runoff events with low RC values. According to Fig. 10, there is a clear gradient of the shapes of ECDFs of RCs from dryer to wetter climate regions. For example, at $\mathrm{RC} = 0.02$, the ECDF of desert climate is around 50 % meaning 50 % of rainfall-runoff events in desert climate region have $\mathrm{RC} < 0.02$. In grassland climate (wetter than desert), the ECDF of $\mathrm{RC} = 0.02$ is roughly 40 %. The ECDF at $\mathrm{RC} = 0.02$ for temperate, subtropical, and tropical climate regions is around 10 % while it decreases to 2 % in equatorial. The similar relationship between RC distribution and climate is observed for other RC values. Although we acknowledge that the number of catchments in equatorial regions are much fewer than others with just 2 catchments, a clear large-scale pattern across Australia emerges: in wetter catchments, during each event rainfall contributes more to runoff, highlighting increasing potential for runoff generation. Studies in other places around the world have shown that the spatial distribution of RCs is strongly correlated with precipitation and align with our findings (Norbiato et al., 2009; Merz and Blöschl, 2009; Merz et al., 2006).

Figure 10 exhibits a climatic signature that can be used to categorize Australian catchments in three different groups across climates based on their dominant runoff generation mechanism. In desert and grassland regions, the ECDF rises sharply at $\mathrm{RC} \approx 0$, indicating that high proportion of rainfall-runoff events produce negligible runoff, meaning rainfall is largely lost due to infiltration and evaporation. This points to less potential for rainfall to produce runoff via saturation excess, and thus suggests the potential dominance of infiltration-excess runoff generation mechanism in these regions. In subtropical, temperate, and equatorial regions, however, the ECDFs rise most gradually towards higher RCs, suggesting a high proportional rainfall becoming runoff in general. This pattern is often seen in regions with greater antecedent soil moisture and the predominance of saturation-excess processes. Tropical catchments show an intermediate pattern: the ECDF increases smoothly from $\mathrm{RC} \approx 0$ and is right-shifted relative to arid zones, indicating a mixed regime of runoff generation. Saturation-excess may dominate during wet periods, while infiltration-excess can occur under high-intensity rainfall (Kidron, 2021; Johnson et al., 2016; Mirus and Loague, 2013; Trancoso et al., 2016). Moreover, runoff events in desert and grassland regions have longer duration than runoff events in temperate, subtropical, and equatorial regions (Fig. 9d) confirming this categorization.

Moving from dryer to wetter catchments, the ECDF of RCs become less skewed (Fig. 10). This is consistent with (Merz and Blöschl, 2009) who reported that RC in dryer catchments is more skewed. RCs between 0 to 0.25 become more evenly distributed moving from dryer to wetter climates. In equatorial climate region, the ECDF of RCs between 0 to 0.25 resemble to follow a uniform distribution. For RCs more than 0.5, the ECDF of RCs almost follows a linear relationship with steeper slope for wetter catchments. The steeper slope of ECDF of RCs in wetter catchments reveals that there is a higher probability of occurrence of hydrologic extremes in wetter catchments which is align with what reported in Norbiato et al. (2009) and Breinl et al. (2021).

5 Discussion

5.1 On the use of the RVEIM

In the process of identifying rainfall-runoff events, the use of parameters to specify "rules" to define events is usu-

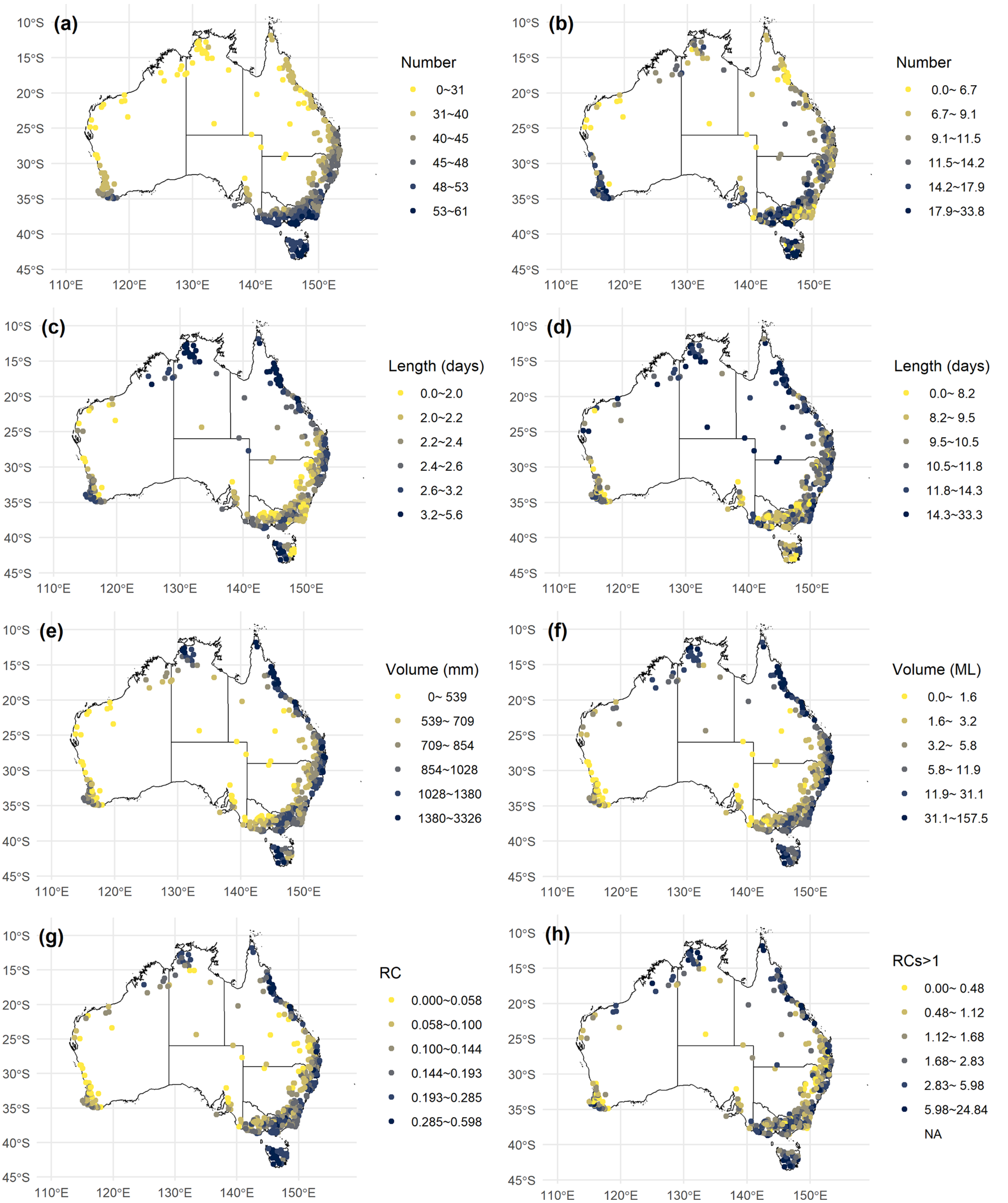

Figure 9. Characteristics of rainfall-runoff event across Australia. **(a)** mean annual number of rainfall events. **(b)** mean annual number of runoff events. **(c)** mean annual length of rainfall events. **(d)** mean annual length of runoff events. **(e)** mean annual volume of rainfall events. **(f)** mean annual volume of runoff events. **(g)** mean runoff coefficient of all rainfall-runoff events. **(h)** mean percentage of rainfall-runoff events with RCs > 1.

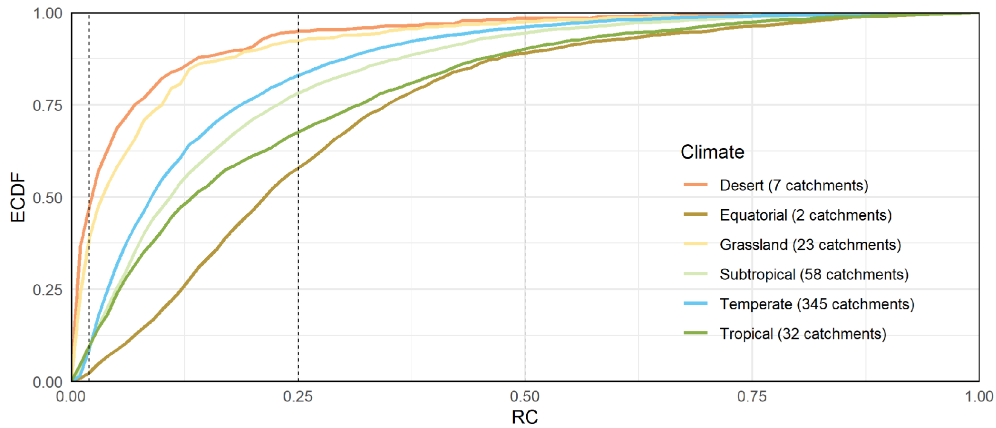

Figure 10. The median ECDF of RCs across HRS catchments grouped by climate regions. The vertical dashed lines, labelled in the figure, mark selected reference RC values of 0.02, 0.25, and 0.5 to facilitate comparison among climate regions.

ally unavoidable, however, decreasing the number of parameters is beneficial for reducing uncertainty (Mohammadpour Khoie et al., 2025). In this study, we presented RVEIM which attempts to address the challenges with conventional rainfall-runoff event identification methods while using a fewer number of parameters. RVEIM's key benefit is incorporating a physical understanding of runoff-generation processes into statistical event identification with the fewest parameters within known methods, which are unlikely to differ across different hydro-climatic conditions, making the method less uncertain and more transferable across different hydro-climatic conditions.

Independence of runoff events is always an important consideration in identifying rainfall-runoff events with parameters used to define periods of time without an event usually used to define independence (Tang and Carey, 2017). Although such parameters might be useful, they increase the uncertainty, as there is no standard to select such a time period, as it may vary between catchments and the events themselves. To address this, RVEIM identifies runoff events based on independent rainfall events; hence it ensures the independence of corresponding runoff events while minimizing the number of parameters.

A threshold value is usually necessary to detect/delineate a runoff event. The threshold, in some cases, is applied directly to the streamflow records (Tang and Carey, 2017; Wasko and Guo, 2022), sometimes to the variance of streamflow data (Fischer et al., 2021), or in other cases, to the rainfall records (Giani et al., 2022). This also adds uncertainty and reduces transferability. For example, in DMCA, a threshold is considered for detecting rainfall events (*rain_min* which is distinct from the peak-over-threshold approach). They showed that change in the threshold value can significantly change the characteristics of identified rainfall-runoff events. They showed that lower values of the threshold lead to fewer but longer and larger rainfall-runoff events, while larger values lead to more but shorter and smaller ones. The variability introduced by threshold value change leads to substantial uncertainty, complicating subsequent analyses.

Compared with the existing approaches, the proposed approach to specify the variance threshold of streamflow is more robust across different climates while relying on less parameters. The proposed approach tries to find the variance of baseflow-dominated streamflow. In RVEIM, there is only one *alpha* parameter which affects the estimation of baseflow, and hence, the variance threshold *var_lim*. To show the robustness of variance threshold against parameter value change, we tested the changes of the average annual number of rainfall-runoff events against changing *alpha* value (*d_var* is fixed). Figure A5 shows the variability of average annual number of rainfall-runoff events across *alpha* values for 8 representative catchments. In all catchments, the variability of average annual number of rainfall-runoff events is low (where the standard deviation for each catchment is within ± 3.48 % of the corresponding mean). This approach to threshold selection enhances the transferability of RVEIM while reducing uncertainty.

RVEIM simultaneously detects and pairs runoff events on the basis of detected rainfall events. The dynamic detection and pairing of rainfall and runoff events has several advantages. By detecting runoff events from rainfall events, RVEIM mirrors the natural hydrologic process. In RVEIM, each rainfall event is matched with its corresponding runoff event (if one can be identified) before moving to the next rainfall event reducing the risk of mispairing. Existing methods vary the direction of pairing (many studies pairing from runoff to rainfall), and they may also vary the statistics used to pair (peak of rainfall/runoff, start/end of rainfall/runoff) (Wasko and Guo, 2022). However, RVEIM considers the temporal runoff generation causality and searches for runoff from the start of each rainfall event.

RVEIM also enhances the way of determining the length of search window and the way of finding corresponding runoff for each rainfall. Conventional methods usually use a time-invariant search window should be defined by the user. Using a time invariant search window may force rainfall-runoff event identification to identify specific types of events, such as shorter runoff events (Mohammadpour Khoie et al., 2025), which may bias towards specific runoff generation mechanism. However, in RVEIM, the length of search window is not user-defined and changes across rainfall events. This allows RVEIM to capture runoff events with various lengths which has higher potential of capturing a fuller range of mechanisms of runoff generation. Moreover, including the length of rainfall in the search window can maximize the probability of correctly capturing multi-peak runoff events. The number of peaks in a runoff event is usually dependent on number of peaks in the corresponding rainfall event and wetness conditions during the runoff event (Tarasova et al., 2018b; Gao et al., 2025); hence, incorporating rainfall length as well as *best_lag* in the search window implicitly considers the temporal pattern of the rainfall and helps ensure that the associated runoff is accurately captured. This also eliminates the parameter usually considered to ensure the independency of two consecutive runoff peaks (Wasko and Guo, 2022).

RVEIM could, in principle, be applied to sub-daily data because its identification rules are based on physically meaningful changes in streamflow. However, because runoff event detection is initiated from independently identified rainfall events, the definition and consistent delineation of rainfall events at sub-daily resolutions would be critical. Although the underlying rules should remain physically applicable, the greater variability and noise at finer temporal resolutions may require adjustments to parameter definitions and thresholds.

5.2 Limitations

The use of RVEIM is still associated with some errors. Although it is challenging to identify errors due to a lack of "ground truth" data, analyzing RC values may help, as RCs > 1 indicate physically implausible events. We must acknowledge that there might be some rainfall-runoff events with valid RC values that are still incorrectly identified or paired, however, a high percentage of rainfall-runoff events with RCs > 1 generally indicates greater errors in rainfall-runoff event identification.

Values of RC ≥ 1 can occur for various reasons. The first reason is overestimation of runoff volume. For some *alpha* values, the baseflow filter may estimate lower baseflow locally/generally which causes an overestimation of runoff volume leading to RCs > 1. This situation is more probable in wet catchments. Wet catchments usually have lower rainfall losses (higher RC values) which increases the probability of RC values exceeding 1. Secondly, in some cases, the rainfall-runoff event identification method may pair a runoff event with the incorrect runoff leading to identifying a rainfall-runoff event with RC > 1. This is, again, more probable in wetter catchments where there is higher number of rainfall and runoff events. When the number of rainfall/runoff events increases, there can be less clear separation of rainfall-runoff events which confuses rainfall-runoff event identification.

Underestimation of rainfall volume is the third potential reason for RCs > 1, most likely due to disinformation in the observations (Beven, 2019). In some cases (especially regions where rainfall is highly spatially variable, such as mountainous regions) not all rainfall events may be captured by the rainfall gauges. In this case, a large volume of runoff might be correctly paired to a small recorded rainfall event, which is actually an underestimate of a larger rainfall event, causing RC to exceed. Here we have assumed rainfall events to be deterministic. However, it may be that two consecutive rainfall events are both part of a single multi-peak event but are separated by a rainfall amount below the 1 mm threshold. In this case the POT detects two smaller rainfall events, and it is probable that one rainfall event is paired to the runoff with the other one left unpaired. However, this can be accommodated through post processing of unpaired rainfall events. Finally, errors in streamflow gauging, rating curve extrapolation, and the use of daily data (which may not accurately capture the timing or dynamics of rainfall-runoff events) can also contribute to RC values exceeding 1 (Beven, 2012) but the impacts of such errors are beyond the scope here.

Considering Fig. 9, catchments which are in regions with more rainfall/runoff events do indeed have higher uncertainty and percentage of RCs > 1. For example, catchment G8150018 has relatively higher percentage of RCs > 1 according to Fig. 7. Tasmanian catchments are usually the worst cases with the highest percentages of RCs > 1, and they satisfy all above-mentioned contributing conditions. For example, catchment 306119 located in western Tasmania where there is high number of rainfall/runoff events, the soil moisture is the highest (Fig. A4), and the elevation is high. In such catchments, improving the temporal resolution of data (i.e. sub-daily data) may enhance the correct identification of rainfall-runoff events but will also likely introduce more noise in the measurements.

5.3 Implications

We used the RVEIM to generate a first Australia-wide summary of rainfall-runoff event characteristics, as well as the distribution of event RCs (Sect. 4.3). Catchments showing a gradual/slow increase of ECDF of RCs at RC ≈ 0 suggest dominance of the saturation-excess runoff process, distinguishing them from those governed by infiltration-excess runoff (sharp increase of ECDF at RC ≈ 0). The results closely align with hydrologic understanding of climate variations in Australia. In northern Australia (tropical and equatorial climates) catchment responses highly vary based on rainfall intensity and soil moisture during wet seasons. So, it is expected to see a wider variety of rainfall-runoff events with various RCs comparing to other regions (Duvert et al., 2022). In the desert climate in Australia, the rainfall losses are high, meaning there is lower potential for catchments in arid climate to generate runoff (Zaman et al., 2012). Therefore, it is expected to see rainfall-runoff events have lower RCs (i.e., ECDF of RCs shifts to left) in Fig. 7. Comparing catchments in different climates, catchments with higher soil moisture and lower actual evapotranspiration are expected to have less rainfall losses and thus higher RCs. ECDFs of RCs obtained from all methods indicate that RVEIM better presents rainfall-runoff relationships (Fig. 8). For example, catchment 306119 in western Tasmania, where soil moisture is extremely high, should generate rainfall-runoff events with relatively high RCs. Among the three methods, the ECDF derived from RVEIM suggests a greater runoff generation potential in the Tasmanian catchment, as it assigns less probability mass to very low RCs than local maxima and DMCA (Fig. 8f). Results are broadly consistent with (Merz et al., 2006) demonstrating that the shape of ECDF of RCs can relate to climatic conditions (such as mean annual rainfall or soil moisture).

More broadly, accurate identification of rainfall-runoff events across the full spectrum of event magnitudes and climates is crucial for characterizing catchment responses at large/national scale. Australia has a highly diverse runoff patterns, ranging from water-limited regions in central Australia to regions with frequent rainfall/runoff events such as Tasmania. Existing rainfall-runoff event identification methods are often highly sensitive to parameter values, which can lead to biased identifying of event characteristics. For example, some settings may capture only very large events (Leenman et al., 2023), while others may force the identification of only short-duration runoff responses (Mohammadpour Khoie et al., 2025) and identification of only a limited number of runoff processes that exist in a catchment (Merz et al., 2006). These biases reduce comparability across regions and may obscure the climatic gradients that shape runoff response. However, the RVEIM provides a more consistent basis for comparing runoff processes across contrasting climates, thus offering a systematic classification of runoff response.

Many regions worldwide face the challenge of understanding hydrological response under changing conditions, whether due to droughts, land-use change, or climate change. As the RVEIM reduces uncertainty and captures both small and large runoff events, it provides a transferable framework for exploring how catchments respond to rainfall in different hydroclimatic settings. Future studies can further investigate the key climatic and catchment-scale drivers of rainfall-runoff event characteristics identified by RVEIM. Linking event-scale characteristics (RC, for example) to such drivers would help explain regional variations in runoff generation. RVEIM can be also used to classify rainfall-runoff events based on dominant runoff mechanisms (e.g., infiltration- versus saturation-excess) and to explore how these behaviors evolve under different hydroclimatic conditions (such as climate change). Such analyses would facilitate systematic understanding of catchment response and enhance predictive rainfall-runoff models at large spatial scales. Using RVEIM, therefore, improves confidence in runoff characteristics used for infrastructure design and flood risk assessment, and allows researchers to better assess how event-scale processes shift under climate change in large sample studies.

6 Conclusion

Various rainfall-runoff event identification methods have been developed using different frameworks to help better characterize rainfall-runoff events. These methods are largely statistical in nature, with the use of parameters inevitable in their use to identify rainfall-runoff events. However, deciding about which parameters values to adopt can be challenging, as not only is there an absence of ground-parameters' for calibration of these methods, changing the parameter values, in most cases, significantly alters the rainfall-runoff event characteristics and hence our understanding of the catchment response.

In this study, we proposed RVEIM, a novel rainfall-runoff event identification method which better mimics the runoff generation process and offers greater robustness compared to current methods. Current rainfall-runoff event identification methods usually detect runoff events and pair them to detected rainfall events. RVEIM, however, detects independent rainfall events, and pairs them to runoff events one by one. On this basis, the number of parameters, as a source of uncertainty, is decreased while ensuring independence of runoff events and detection of multi-peak events. Additionally, the one-by-one pairing of rainfall and runoff events decreases the potential of wrong pairing which is responsible for identifying physically implausible rainfall-runoff events (e.g., generating RCs > 1) and disturbing our understanding about hydrologic regime in a catchment.

We applied RVEIM to 467 unimpacted catchments across Australia meaning a mostly natural runoff generation is observed. Results of RVEIM demonstrated that the method generally performs well across different climate regions in Australia. Assessing uncertainty of parameter value change showed that the use of RVEIM results in a more confident characterization of rainfall-runoff events in all catchments. For example, for 90 % of catchments in Australia, the maximum percentage of RCs > 1 was 6 %, much lower than those obtained using the benchmarking rainfall-runoff event identification methods. The ECDFs of RCs obtained from RVEIM and the benchmarking rainfall-runoff event identification methods in various catchments demonstrated that the results of the proposed rainfall-runoff event identification method are more aligned with the hydrologic understandings in catchment.

Using RVEIM, we compiled a first, comprehensive summary of rainfall-runoff event characteristics across Australian catchments. Results showed that the distribution of RCs gradually differs moving across climates – moving from drier to wetter catchments the ECDF of RCs shift from sharper to more gradual curves – highlighting a systematic increase in the RCs across rainfall-runoff events and thus higher potential of runoff generation. Moreover, it was shown that the distribution of RCs become more uniform when moving towards wetter catchments. Results of this study lead to better understanding of rainfall-runoff relationships in Australian catchments and, with the proposed method performing well across the diverse range of climate, RVEIM is likely transferable to catchments in other regions globally.

Appendix A

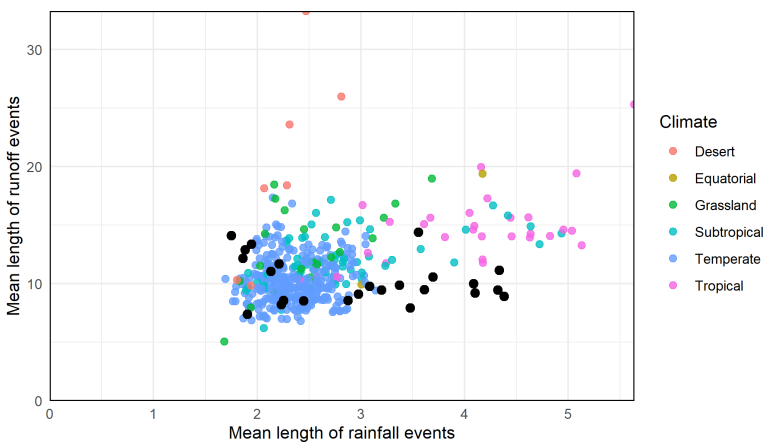

Figure A1. Mean length of rainfall versus runoff events for each catchment. Black dots show catchments in Tasmania.

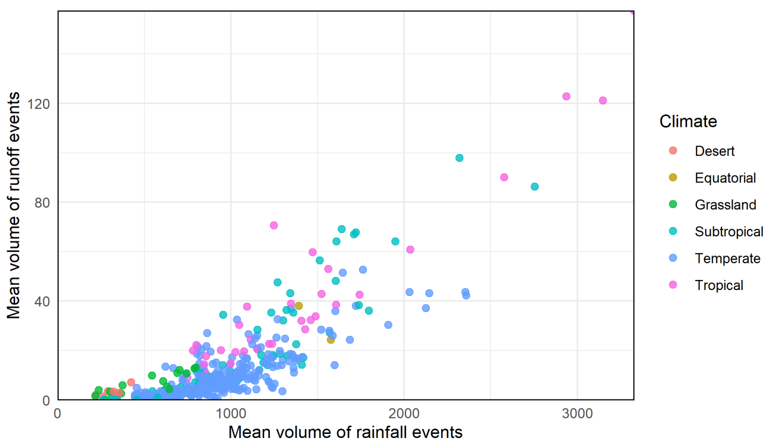

Figure A2. Mean volume of rainfall versus runoff events for each catchment.

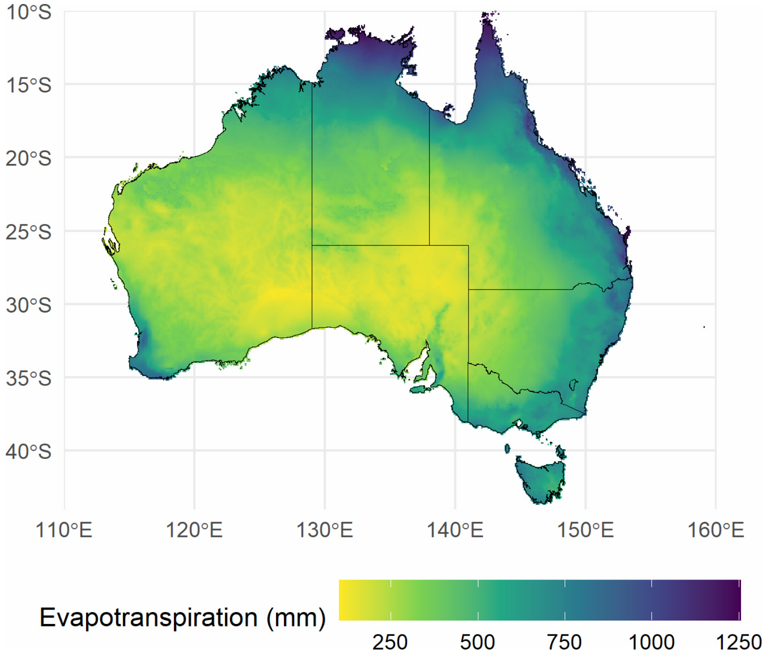

Figure A3. Spatial distribution of mean annual evapotranspiration across Australia.

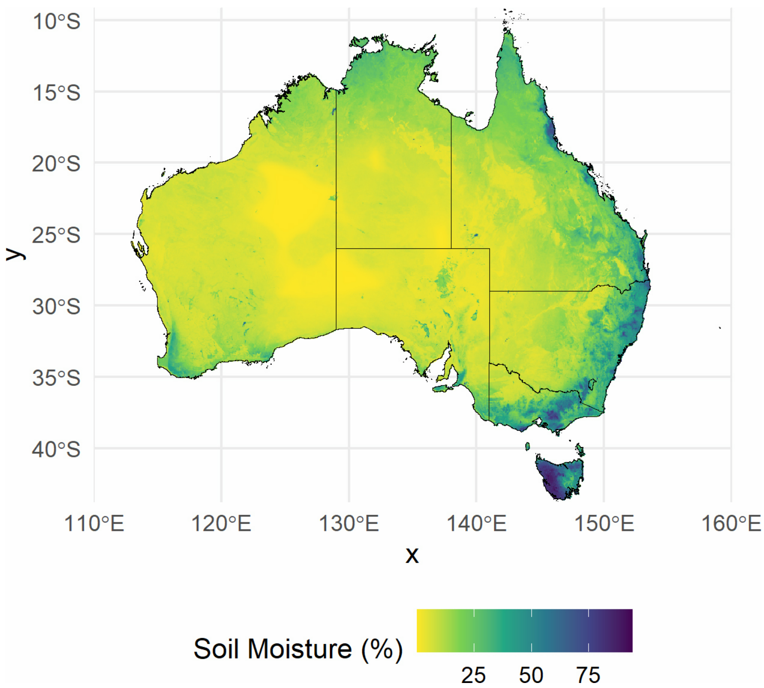

Figure A4. Spatial distribution of mean soil moisture across Australia.

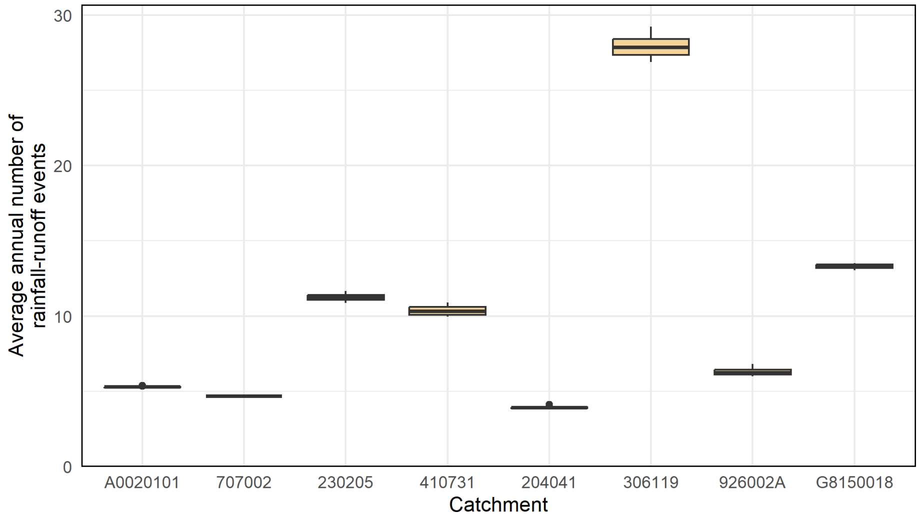

Figure A5. Boxplot of the average annual number of rainfall-runoff events.

Code availability. The new event identification and pairing method developed is published as a function named *eventRVEIM* within the R package *hydroEvents* (ver. 0.13.0), accessible via CRAN: https://cran.r-project.org/web/packages/hydroEvents/index.html (last access: 8 September 2026).

Data availability. All data used in this study were sourced from public repositories as detailed in Sect. 2. Streamflow from the Bureau of Meteorology's Hydrologic Reference Stations (Bureau of Meteorology, 2025a), and rainfall, evapotranspiration, and soil moisture from the Bureau of Meteorology's Australian Water Availability Project (AWAP) (Jones et al., 2009) available at https://thredds.nci.org.au/thredds/catalog/catalogs/zv2/agcd/agcd.html (last access: 8 September 2026).

Author contributions. Mohammad Masoud Mohammadpour Khoie: Writing – review & editing, Writing – original draft, Visualization, Validation, Software, Resources, Project administration, Methodology, Investigation, Formal analysis, Data curation, Conceptualization. Danlu Guo: Writing – review & editing, Visualization, Validation, Supervision, Resources, Project administration, Methodology, Funding acquisition, Data curation, Conceptualization. Conrad Wasko: Writing – review & editing, Visualization, Validation, Supervision, Resources, Project administration, Methodology, Data curation, Conceptualization.

Competing interests. The contact author has declared that none of the authors has any competing interests.

Acknowledgements. We acknowledge the National Computational Infrastructure (NCI), supported by the Australian Government, for providing high-performance computing resources. Dr. Conrad Wasko is supported by the Sydney Horizon Fellowship at the University of Sydney.

Review statement. This paper was edited by Thom Bogaard and reviewed by two anonymous referees.

References

Amirthanathan, G. E., Bari, M. A., Woldemeskel, F. M., Tuteja, N. K., and Feikema, P. M.: Regional significance of historical trends and step changes in Australian streamflow, Hydrol. Earth Syst. Sci., 27, 229–254, https://doi.org/10.5194/hess-27-229-2023, 2023.

Ashcroft, L., Karoly, D. J., and Dowdy, A. J.: Historical extreme rainfall events in southeastern Australia, Weather and Climate Extremes, 25, 100210, https://doi.org/10.1016/j.wace.2019.100210, 2019.

Beven, K.: Towards a methodology for testing models as hypotheses in the inexact sciences, P. R. Soc. A, 475, 20180862, https://doi.org/10.1098/rspa.2018.0862, 2019.

Beven, K. J.: Rainfall-runoff modelling: the primer, John Wiley & Sons, https://doi.org/10.1002/9781119951001, 2012.

Breinl, K., Lun, D., Müller-Thomy, H., and Blöschl, G.: Understanding the relationship between rainfall and flood probabilities through combined intensity-duration-frequency analysis, J. Hydrol., 602, 126759, https://doi.org/10.1016/j.jhydrol.2021.126759, 2021.

Bureau of Meteorology: Hydrologic Reference Stations, http://www.bom.gov.au/water/hrs/ (last access: 8 September 2026), 2025a.

Bureau of Meteorology: Average annual and monthly evapotranspiration maps: http://www.bom.gov.au/climate/maps/averages/evapotranspiration/ (last access: 8 September 2026), 2025b.

Bureau of Meteorology: Australian Water Outlook: https://awo.bom.gov.au/products/historical/soilMoisture-rootZone/ (last access: 8 September 2026), 2025c.

Chen, L., Liu, C., Li, Y., and Wang, G.: Impacts of climatic factors on runoff coefficients in source regions of the Huanghe River, Chinese Geogr. Sci., 17, 047-055, https://doi.org/10.1007/s11769-007-0047-4, 2007.

Chen, X., Parajka, J., Széles, B., Valent, P., Viglione, A., and Blöschl, G.: Impact of climate and geology on event runoff characteristics at the regional scale, Water, 12, 3457, https://doi.org/10.3390/w12123457, 2020.

Douinot, A., Iffly, J. F., Tailliez, C., Meisch, C., and Pfister, L.: Flood patterns in a catchment with mixed bedrock geology and a hilly landscape: identification of flashy runoff contributions during storm events, Hydrol. Earth Syst. Sci., 26, 5185–5206, https://doi.org/10.5194/hess-26-5185-2022, 2022.

Duvert, C., Lim, H.-S., Irvine, D. J., Bird, M. I., Bass, A. M., Tweed, S. O., Hutley, L. B., and Munksgaard, N. C.: Hydrological processes in tropical Australia: Historical perspective and the need for a catchment observatory network to address future development, J. Hydrol.-Regional Studies, 43, 101194, https://doi.org/10.1016/j.ejrh.2022.101194, 2022.

Fischer, S. and Schumann, A. H.: Temporal changes in the frequency of flood types and their impact on flood statistics, J. Hydrol. X, 22, 100171, https://doi.org/10.1016/j.hydroa.2024.100171, 2024.

Fischer, S., Schumann, A., and Bühler, P.: A statistics-based automated flood event separation, J. Hydrol. X, 10, 100070, https://doi.org/10.1016/j.hydroa.2020.100070, 2021.

Gao, H., Pfister, L., and Kirchner, J. W.: Quantifying controls on rapid and delayed runoff response in double-peak hydrographs using ensemble rainfall-runoff analysis (ERRA), Hydrol. Earth Syst. Sci., 29, 6529–6547, https://doi.org/10.5194/hess-29-6529-2025, 2025.

Giani, G., Tarasova, L., Woods, R. A., and Rico-Ramirez, M. A.: An objective time-series-analysis method for rainfall-runoff event identification, Water Resour. Res., 58, e2021WR031283, https://doi.org/10.1029/2021WR031283, 2022.

Guo, D., Zheng, F., Gupta, H., and Maier, H. R.: On the Robustness of Conceptual Rainfall-Runoff Models to Calibration and Evaluation Data Set Splits Selection: A Large Sample Investigation, Water Resour. Res., 56, e2019WR026752, https://doi.org/10.1029/2019WR026752, 2020.

Ho, M., Nathan, R., Wasko, C., Vogel, E., and Sharma, A.: Projecting changes in flood event runoff coefficients under climate change, J. Hydrol., 615, 128689, https://doi.org/10.1016/j.jhydrol.2022.128689, 2022.

Hu, C., Ran, G., Li, G., Yu, Y., Wu, Q., Yan, D., and Jian, S.: The effects of rainfall characteristics and land use and cover change on runoff in the Yellow River basin, China, J. Hydrol. Hydromech., 69, 29–40, 2021.

Johnson, F., White, C. J., van Dijk, A., Ekstrom, M., Evans, J. P., Jakob, D., Kiem, A. S., Leonard, M., Rouillard, A., and Westra, S.: Natural hazards in Australia: floods, Climatic Change, 139, 21–35, https://doi.org/10.1007/s10584-016-1689-y, 2016.

Jones, D. A., Wang, W., and Fawcett, R.: High-quality spatial climate data-sets for Australia, Aust. Meteorol. Ocean., 58, 233–248, https://doi.org/10.22499/2.5804.003, 2009.

Kaur, S., Horne, A., Stewardson, M. J., Nathan, R., Costa, A. M., Szemis, J. M., and Webb, J. A.: Challenges for determining frequency of high flow spells for varying thresholds in environmental flows programmes, Journal of Ecohydraulics, 2, 28–37, https://doi.org/10.1080/24705357.2016.1276418, 2017.

Kemp, D. and Alankarage, G. H.: Benchmarking three event-based rainfall-runoff routing models on Australian catchments, Hydrology, 10, 131, https://doi.org/10.3390/hydrology10060131, 2023.

Kidron, G. J.: Comparing overland flow processes between semiarid and humid regions: Does saturation overland flow take place in semiarid regions?, J. Hydrol., 593, 125624, https://doi.org/10.1016/j.jhydrol.2020.125624, 2021.

Koskelo, A. I., Fisher, T. R., Utz, R. M., and Jordan, T. E.: A new precipitation-based method of baseflow separation and event identification for small watersheds ($< 50\,km^2$), J. Hydrol., 450, 267–278, 2012.

Ladson, A. R., Brown, R., Neal, B., and Nathan, R.: A Standard Approach to Baseflow Separation Using The Lyne and Hollick Filter, Australasian Journal of Water Resources, 17, 25–34, https://doi.org/10.7158/13241583.2013.11465417, 2013.

Leenman, A. S., Slater, L. J., Dadson, S. J., Wortmann, M., and Boothroyd, R.: Quantifying the Geomorphic Effect of Floods Using Satellite Observations of River Mobility, Geophys. Res. Lett., 50, e2023GL103875, https://doi.org/10.1029/2023GL103875, 2023.

Lyne, V. and Hollick, M.: Stochastic Time-Variable Rainfall-Runoff Modeling, Institute of Engineers Australia National Conference, https://www.researchgate.net/publication/272491803_Stochastic_Time-Variable_Rainfall-Runoff_Modeling (last access: 8 September 2026), 1979.

Mei, Y., Wang, D., Zhu, J., Tang, G., Cai, C., Shen, X., Hong, Y., and Zhang, X.: Optimal Baseflow Separation Through Chemical Mass Balance: Comparing the Usages of Two Tracers, Two Concentration Estimation Methods, and Four Baseflow Filters, Water Res. Res., 60, e2023WR036386, https://doi.org/10.1029/2023WR036386, 2024.

Merz, R. and Blöschl, G.: A regional analysis of event runoff coefficients with respect to climate and catchment characteristics in Austria, Water Resour. Res., 45, https://doi.org/10.1029/2008WR007163, 2009.

Merz, R., Blöschl, G., and Parajka, J.: Spatio-temporal variability of event runoff coefficients, J. Hydrol., 331, 591–604, https://doi.org/10.1016/j.jhydrol.2006.06.008, 2006.

Metcalfe, R. and Schmidt, B.: Streamflow Analysis and Assessment Software, Version 4.1, Ontario Ministry of Natural Resources and Forestry [code], Peterborough, ON, Canada, http://people.trentu.ca/rmetcalfe/SAAS.html (last access: 8 September 2026), 2016.

Miao, C., Zheng, H., Jiao, J., Feng, X., Duan, Q., and Mpofu, E.: The changing relationship between rainfall and surface runoff on the Loess Plateau, China, J. Geophys. Res.-Atmos., 125, e2019JD032053, https://doi.org/10.1029/2019JD032053, 2020.

Mirus, B. B. and Loague, K.: How runoff begins (and ends): Characterizing hydrologic response at the catchment scale, Water Resour. Res., 49, 2987–3006, https://doi.org/10.1002/wrcr.20218, 2013.

Mohammadpour Khoie, M. M., Guo, D., and Wasko, C.: Improving the consistency of hydrologic event identification, Environ. Modell. Softw., 191, 106521, https://doi.org/10.1016/j.envsoft.2025.106521, 2025.

Nathan, R., Jordan, P., Scorah, M., Lang, S., Kuczera, G., Schaefer, M., and Weinmann, E.: Estimating the exceedance probability of extreme rainfalls up to the probable maximum precipitation, J. Hydrol., 543, 706–720, https://doi.org/10.1016/j.jhydrol.2016.10.044, 2016.

Nathan, R. J. and McMahon, T. A.: Evaluation of automated techniques for base flow and recession analyses, Water Resour. Res., 26, 1465–1473, https://doi.org/10.1029/WR026i007p01465, 1990.

Nathan, R. J. and McMahon, T. A.: Recommended practice for hydrologic investigations and reporting, Australian Journal of Water Resources, 21, 3–19, https://doi.org/10.1080/13241583.2017.1362136, 2017.

Norbiato, D., Borga, M., Merz, R., Blöschl, G., and Carton, A.: Controls on event runoff coefficients in the eastern Italian Alps, J. Hydrol., 375, 312–325, https://doi.org/10.1016/j.jhydrol.2009.06.044, 2009.

Peterson, T. J., Wasko, C., Saft, M., and Peel, M. C.: AWAPer: An R package for area weighted catchment daily meteorological data anywhere within Australia, Hydrol. Process., 34, 1301–1306, https://doi.org/10.1002/hyp.13637, 2020.

Rahi, A., Rahmati, M., Dari, J., Saltalippi, C., Brogi, C., and Morbidelli, R.: Unraveling hydroclimatic forces controlling the runoff coefficient trends in central Italy's Upper Tiber Basin, J. Hydrol.: Regional Studies, 50, 101579, https://doi.org/10.1016/j.ejrh.2023.101579, 2023.

Schoener, G. and Stone, M. C.: Impact of antecedent soil moisture on runoff from a semiarid catchment, J. Hydrol., 569, 627–636, https://doi.org/10.1016/j.jhydrol.2018.12.025, 2019.

Sillanpää, N. and Koivusalo, H.: Impacts of urban development on runoff event characteristics and unit hydrographs across warm and cold seasons in high latitudes, J. Hydrol., 521, 328–340, https://doi.org/10.1016/j.jhydrol.2014.12.008, 2015.

Song, S. and Wang, W.: Impacts of antecedent soil moisture on the rainfall-runoff transformation process based on high-resolution observations in soil tank experiments, Water, 11, 296, https://doi.org/10.3390/w11020296, 2019.

Sriwongsitanon, N. and Taesombat, W.: Effects of land cover on runoff coefficient, J. Hydrol., 410, 226–238, https://doi.org/10.1016/j.jhydrol.2011.09.021, 2011.

Stern, H., De Hoedt, G., and Ernst, J.: Objective classification of Australian climates, Aust. Meteorol. Mag., 49, 87–96, 2000.

Tang, W. G. and Carey, S. K.: HydRun: A MATLAB toolbox for rainfall-runoff analysis, Hydrol. Process., 31, 2670–2682, https://doi.org/10.1002/hyp.11185, 2017.

Tarasova, L., Basso, S., Poncelet, C., and Merz, R.: Exploring Controls on Rainfall-Runoff Events: 2. Regional Patterns and Spatial Controls of Event Characteristics in Germany, Water Resour. Res., 54, 7688–7710, https://doi.org/10.1029/2018WR022588, 2018a.

Tarasova, L., Basso, S., Zink, M., and Merz, R.: Exploring Controls on Rainfall-Runoff Events: 1. Time Series-Based Event Separation and Temporal Dynamics of Event Runoff Response in Germany, Water Resour. Res., 54, 7711–7732, https://doi.org/10.1029/2018WR022587, 2018b.

Tarasova, L., Basso, S., and Merz, R.: Transformation of generation processes from small runoff events to large floods, Geophys. Res. Lett., 47, e2020GL090547, https://doi.org/10.1029/2020GL090547, 2020.

Trancoso, R., Larsen, J. R., McAlpine, C., McVicar, T. R., and Phinn, S.: Linking the Budyko framework and the Dunne diagram, J. Hydrol., 535, 581–597, https://doi.org/10.1016/j.jhydrol.2016.02.017, 2016.

Voloh, B., Watson, M. R., König, S., and Womelsdorf, T.: MAD saccade: Statistically robust saccade threshold estimation via the median absolute deviation, Journal of Eye Movement Research, 12, https://doi.org/10.16910/jemr.12.8.3, 2020.

Wang, S., Zhang, Z., McVicar, T. R., Zhang, J., Zhu, J., and Guo, J.: An event-based approach to understanding the hydrological impacts of different land uses in semi-arid catchments, J. Hydrol., 416–417, 50–59, https://doi.org/10.1016/j.jhydrol.2011.11.035, 2012.

Wasko, C. and Guo, D.: Understanding event runoff coefficient variability across Australia using the hydroEvents R package, Hydrol. Process., 36, e14563, https://doi.org/10.1002/hyp.14563, 2022.

Wasko, C., Guo, D., Ho, M., Nathan, R., and Vogel, E.: Diverging projections for flood and rainfall frequency curves, J. Hydrol., 620, 129403, https://doi.org/10.1016/j.jhydrol.2023.129403, 2023.

Wu, Q., Xie, T., Liu, C., Li, W., Zhang, L., Ran, G., Xu, Y., Tang, Y., Han, Z., and Hu, C.: Improving the understanding of rainfall-runoff processes: Temporal dynamic of event runoff response in Loess Plateau, China, J. Environ. Manage., 375, 123436, https://doi.org/10.1016/j.jenvman.2024.123436, 2025.

Zaman, M. A., Rahman, A., and Haddad, K.: Regional flood frequency analysis in arid regions: A case study for Australia, J. Hydrol., 475, 74–83, https://doi.org/10.1016/j.jhydrol.2012.08.054, 2012.

Zhang, X., Alexander, L., Hegerl, G. C., Jones, P., Tank, A. K., Peterson, T. C., Trewin, B., and Zwiers, F. W.: Indices for monitoring changes in extremes based on daily temperature and precipitation data, WIREs Clim. Change, 2, 851–870, https://doi.org/10.1002/wcc.147, 2011.